Two-Stage Electric Vehicle Charging Optimization Model Considering Dynamic Virtual Price-Based Demand Response and A Hierarchical Non-Cooperative Game

Lin, Hongyu; Dang, Jialu ; Zheng, Haowei ; Yao, Lujin ; Yan, Qingyou ; Yang, Shenbo ; Guo, Hongzhen ; Anvari-Moghaddam, Amjad

Published in:
Sustainable Cities and Society

DOI (link to publication from Publisher):
https://doi.org/10.1016/j.scs.2023.104715

Publication date:
2023

Document Version
Accepted author manuscript, peer reviewed version

Two-Stage Electric Vehicle Charging Optimization Model Considering Dynamic Virtual Price-Based Demand Response and A Hierarchical Non-Cooperative Game

Hongyu Lin[1,2], Jialu Dang[1,2], Haowei Zheng[3], Lujin Yao[4], Qingyou Yan[1,2,*], Shenbo Yang[5,*], Hongzhen Guo[1], Amjad Anvari-Moghaddam[6]

1 School of Economics & Management, North China Electric Power University, Beijing 102206, China

2 Beijing Key Laboratory of New Energy & Low Carbon Development, North China Electric Power University, Beijing 102206, China

3 State Grid Economic and Technological Research Institute Co. LTD, Beijing 102209, China

4 School of Control and Computer Engineering, North China Electric Power University, Beijing 102206, China

5 College of Economics and Management, Beijing University of Technology, Beijing 100124, China

6 Department of Energy (AAU Energy), 9220 Aalborg, Denmark

* Corresponding Author

ABSTRACT: This paper proposes a two-stage bi-layer game charging optimization model based on the background of non-coordination between a distribution network operator (NO), a distributed generation operator (DGO), and a charging agent (CA). In the first stage, a dynamic virtual price-based demand response (DVPBDR) model is constructed to pre-optimize the charging load with the virtual charging cost as the objective. In the second stage, a strategy for adjusting output deviations based on a bi-layer Stackelberg game model is established, with the economic benefits of each participant as the objectives. Full cooperation mode and bi-layer mixed game are introduced to compare with the bi-layer Stackelberg game in Simulation Analysis. The calculation results show that: (1) the DVPBDR is not constrained by the actual electricity price system and mechanism, and reflect the real influence of price changes on charging demands, thus effectively reducing energy abandonment by 41.76% and net load fluctuation by 53.50%; (2) in the full cooperation mode, there is a conflict of interests and CA suffers financial loss, thus resulting in a reduction in comprehensive benefits by at least 61.08%, compared to the non-cooperative cases; (3) in the bi-layer mixed games, the cooperative gain of DGO and NO is superior than that of the cooperation between DGO and CA, so a relative win-win is achieved in the bi-layer mixed game with DGO-CA cooperation, and the comprehensive benefits is increased by 3.32%; (4) in the bi-layer Stackelberg game, each participant has a completely independent awareness of decision-making and establishes strategies for maximizing its own interests, which results in achieving the optimal comprehensive benefits (increases by at least 44.18% compared to other cases). Therefore, multi-dimensional benefits are realized in the multi-participant charging system with a bi-layer Stackelberg game.

KEYWORDS: Electric vehicles (EV); day-ahead and intraday charging optimization; network, generation, and user sides; dynamic virtual price-based demand response, bi-layer Stackelberg game

1 Introduction

1.1 Motivation

With the proposal of "double carbon" goal and the construction of new-type power system in China, clean energy generation (such as wind and solar power) and flexible load resources (such as EVs) have become key concerns and difficulties [1]. On the one hand, Wind and PV power generation are highly uncertain and volatile, which are difficult to control [2]; on the other hand, large-scale charging of EVs enlarges the peak-valley difference of load, which may cause superposition of peaks [3]. Multi-stage and multi-level scheduling management is one of the ways to alleviate the deviation problem of renewables output, by which the operation strategy keeps changing in time based on producible capacity in phrases to reduce power supply deviation [4]. To reduce the supply strain caused by disorderly charging, price guidance can be made full use of to take advantage of the flexibility of EVs. The charging plan can be adjusted following the change of power output, so that orderly charging and renewables output can be coordinated and linked [5]. To address the problem of disordered charge and renewable power consumption, various forms of business modes have been developed [6-8]. Different combinations of operation entities, energy trading modes, and profit models can produce different benefits. Therefore, how to match operation entities, select appropriate trading modes, and establish effective operating strategies to make orderly charging fully consume excess wind and solar power generation, whilst giving consideration to the interests of multiple participants is an urgent problem to be solved at present.

1.2 Literature review

Research on EV charging optimization can be broadly categorized into three main areas: optimizing EV scheduling to maximize the benefits of charging stations [9-11], integrating EVs with clean energy generation to reduce energy wastage and gain economic benefits [12-14], and managing EV charging in an orderly manner to reduce peak demand on distribution networks [15-17]. These areas of research have established a solid foundation for the current study. In this context, the paper considers the interactions between three key players: the distribution network, distributed generation operator, and EVs, in order to develop a multi-operator optimization framework.

Several studies have investigated the optimization of orderly charging by considering the network, generation, and load simultaneously. Lin et al. [18] formulated a multi-objective problem for planning the distribution network, which included the measurement and allocation of distributed generators, shunt capacitors, and charging stations. The problem aimed to improve the secondary power factor, reduce active power losses, and enhance the voltage specifications of the distribution system. Wang et al. [19] constructed a multi-objective model that considered both ordered charge and discharge control. The model aimed to maximize benefits for users, PV generators, and distribution network operators by achieving "peak shaving" and received significant profitability feedback. Wang et al. [20] developed a spatial-temporal two-level scheduling model for EV charging and discharging, which considered the optimal interests of generators, network operators, and users. The model smoothed out load fluctuations, reduced user charging costs on a time scale, and lowered network losses and generation fuel costs on a spatial scale. Sun [21] considered the compatibility between EV participation in auxiliary services and driving demand based on the network-source-load interaction scenario. A robust optimization strategy for EV participation in

wind power standby services was constructed, which solved the impact of wind power uncertainty on the scheduling plan. It was demonstrated that EV participation in wind power standby could effectively reduce the system's dependence on traditional thermal power standby and improve the overall operating economy of the system. Hou et al. [22] constructed a multi-objective generation-network-load optimization model for a microgrid with EV charging and discharging. The objectives were to maximize renewable energy generation in the generation layer, minimize the cost of diesel generation and main network contact line power operation in the network layer, and maximize the economic benefits of EVs in the load layer. This approach ensured economic, safety, and high-efficiency effects for the vehicle fleet, microgrid, and main network. While the above literature confirms the importance of EV charging scheduling in the network-generation-load multi-participant system, these studies tend to focus on multi-objective and cooperative optimization, disregarding the differences among network, generation, and load sides. Thess approaches weaken the autonomous decision-making ability and interest opposition of each operator.

Regarding the optimization of EV charging considering the independence of operating entities, several studies have employed Stackelberg game theory. Yoshihara and Namerikawa [23] dealt with the charging scheduling optimization problem for EVs on highways, where the charging station acted as the leader and the vehicles were the followers. The results showed the superiority of Stackelberg equilibrium over Nash equilibrium. Dai et al. [24] constructed a "one-leader with multi-follower" game model for EV charging optimization, in which the charging station with a PV generator was the leader who aimed to gain maximum profit, and the EV drivers were the followers who intended to minimize charging cost and maximize charging utility. The results showed better performance of the proposed model on profitability. These studies utilize Stackelberg game to construct an orderly charging scheduling model that takes into account dual participants, solving the economic and environmental benefits of users and charging stations when the players have independent consciousness. However, the constructed dual-player system does not consider network operators' interests and is considered as a single-layer Stackelberg game model. Furthermore, previous works on hierarchical Stackelberg game (known as bi-layer Stackelberg game) optimization model (involving three or more participants), such as those conducted by Li et al. [25], Lin et al. [26], Li et al. [27], Luo et al. [28], and Yu et al. [29], were not aimed at charging optimization with consideration of the characteristics of EVs who exhibit individual differences in terms of charging demands, start time, and departure time, etc.

Virtual price is a type of price signaling mechanism used in demand response programs [30]. This mechanism incentivizes users to actively participate in peak shaving and valley filling to promote the consumption of renewables [31]. Ji et al. [30] proposed a virtual real-time pricing model based on time-of-use price and power credit, and their results showed that this demand response mechanism was effective in peak regulation. Xia et al. [32] demonstrated that a virtual time-varying price could help the system coordinate users' behaviors and achieve demand management targets by shaving peaks. Yang et al. [33] applied the virtual price mechanism to an EV-integrated distribution system, and constructed an optimal charging and discharging scheduling model to achieve peak shaving and valley filling. Sun et al. [31] introduced the concept of the "unbalance degree of supply and demand" and used the virtual price mechanism to arrange the charge and discharge of EVs, not only shaving peaks but also increasing PV consumption. While virtual price mechanism is mostly considered as a regulatory tool, only Sun et al. [31] applied it for increasing renewable consumption. However, Sun et al. [31] did not provide a clear explanation of the calculation of virtual price, nor

did they analyze the response of individual EV users to the virtual price.

1.3 Contributions

In light of the reviewed literature, some research gaps are identified as follows:

(1) Current studies on optimizing EV charging with multiple participants tend to overlook the independent decision-making processes and competing interests of network operators, distributed power suppliers, and users. The competitive relationships among these stakeholders are not adequately considered in the optimization process, and there has been little investigation into the optimization effects of multi-player, non-cooperative gaming between the network, generation, and user sides;

(2) Most research on the application of virtual price focuses on the regulating performance of virtual price in managing power fluctuations, but little attention has been paid to the potential value of virtual price in promoting clean energy consumption. Furthermore, for EV users, there are significant individual differences in terms of parking time, dwelling period, and departure time. However, current research tends to treat users as a homogeneous group, and the impact of individual differences on the optimization process has not been explored.

Therefore, the contributions of this paper are summarized as follows:

(1) This study proposes a DVPBDR approach that considers the concept of net load. By treating net load (i.e., the difference between the original load and the output of wind and solar power) as a variable, the virtual price is used to address the problem of wind and PV power abandonment, and a DVPBDR model is developed. To account for user differences, the virtual price is dynamically updated with each user's travel and charging information as input. The virtual charging cost is then used as the optimization objective to create differentiated charging plans for each EV user, thereby minimizing the negative impact of user diversity on optimization results. The approach provides a personalized response strategy reference for EV users with diverse characteristics.

(2) This study constructs a bi-layer non-cooperative Stackelberg game model that involves three levels of participants: the distribution network operator (NO), distributed generation operator (DGO), and charging agent (CA), representing the network side, generation side, and load side, respectively. The NO is considered the top level, the DGO as the middle level, and the CA as the bottom level. In the upper-layer game, the NO is the leader, and the DGO is the follower, while in the lower layer, the DGO is the leader, and the CA is the follower. Through continuous information exchange and iterative competition, the study establishes an optimal balanced scheme that takes into account the interests of all three players. The model provides a new idea of charging scheduling optimization for participants (suppliers or consumers) with independent decision-making ability.

(3) This study establishes a two-stage operation mode for a multi-player system, considering power generation uncertainty. The approach employs scenario generation and reduction methods to handle the uncertainty of wind and solar power generation and determine day-ahead and intraday power generation curves. In the day-ahead stage, the DVPBDR model is utilized to pre-optimize the charging load to absorb wind and solar generation to the greatest extent possible. In the intraday stage, a hierarchical Stackelberg game is employed to flexibly adjust the charging demand of EVs, minimizing the impact of power generation bias. The mode enables a multi-time scale charging optimization application with EV flexibility to address renewable output deviations.

1.4 Organization of this paper

The rest of this paper is organized as follows: Section 2 constructs a multi-operator two-stage operation system structure and related models (including uncertainty modeling of renewable energy and EV charging load modeling); Section 3 builds a two-stage operation optimization model, including a day-ahead operation optimization model based on the DVPBDR and an intraday bi-layer Stackelberg game optimization model based on three operators. Section 4 conducts a case analysis. Finally, section 5 concludes this paper.

2 Structure and modeling of multiple operator-involved charging system

2.1 System framework under two-stage operation mode

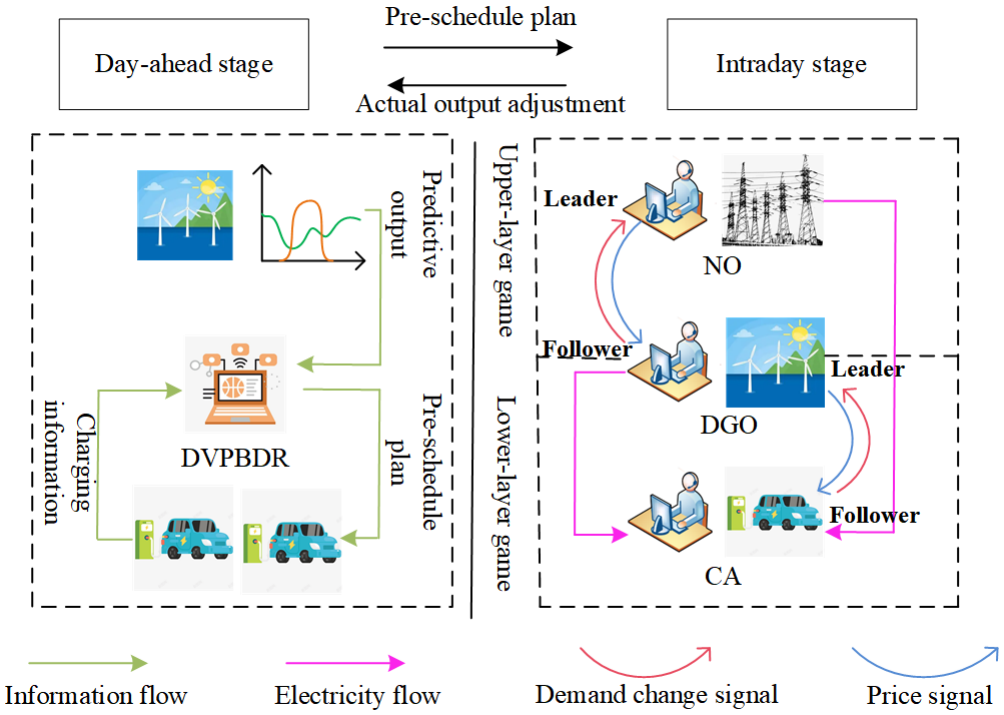

Figure 1 System structure and operation framework

The charging system and operational framework proposed in this paper is shown in Figure 1.

This charging system involves three independent operators: the NO, DGO, and CA. The DGO, which is powered by wind and PV generators, serves as the primary energy supplier. If demand exceeds the DGO's capacity, the NO, which relies on thermal power, supplies the remaining energy. The CA is responsible for managing user charging.

In the two-stage operation mode, the DGO predicts the solar and wind power generation for the next day in the day-ahead stage. The CA collects the charging information from users and reports it to the DGO. Using the DVPBDR model, the DGO determines the charging plans for the second day and provides feedback to the CA to complete the day-ahead scheduling preparation. In the intraday stage, the DGO measures the actual solar and wind power generation for the day and

transmits a price signal to the CA due to the deviation from the forecast. The CA adjusts the charging demand and provides a new charging plan to the DGO. If the demand cannot be met, the DGO reports the unmet load to the NO (who adjusts the selling price) to purchase the electricity from the NO, and finally a power purchase agreement is reached. The whole process in intraday is based on the bi-layer Stackelberg game.

2.2 Uncertainty modeling of wind and PV power generation

Renewable energies in this system consist of wind power and PV, and their uncertainty is modeled using scenario generation and reduction methods (see Appendix for details). The Latin hypercube sampling method [34] is used for scenario generation, and scenario reduction is based on [35]. Appendix also includes output models for wind power [36] and PV power [37].

2.3 Charging demand modeling of EVs

The individual differences of users are reflected in the charging demand of EV users (related to initial state-of-charge (SOC), remaining SOC, travel mileage, and energy consumption) and the parking period (arrival and departure time at the charging station), etc.

2.3.1 Mileage fitting

The mileage of each trip follows a lognormal distribution, which is given by:

$$d = \frac{1}{x\sigma\sqrt{2\pi}} \cdot e^{-\frac{(\ln x-\mu)^2}{2\sigma^2}} \tag{1}$$

where μ is the mean value, σ is the standard deviation. Based on NHTS2017 dataset [38], we obtained the results $\mu = 1.2051, \sigma = 1.2766$, as shown in Figure 2.

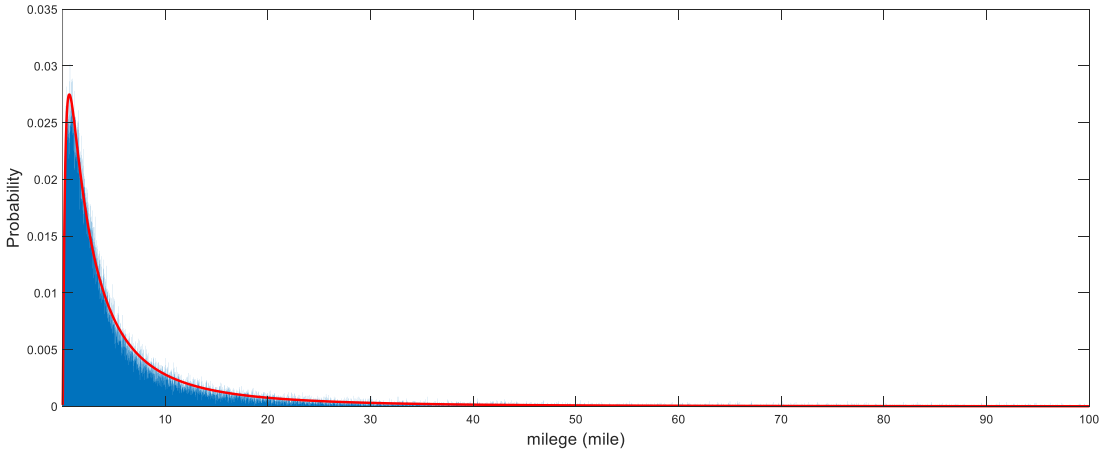

Figure 2 Mileage fitting results

2.3.2 Power consumption

According to [39], the energy consumption model of an EV can be obtained by calculating the energy consumption per unit distance at different driving speeds. The energy efficiency is related to the driving speed. The details are as follows:

$$e = 0.21 - 0.001v + \frac{1.531}{v} \tag{2}$$

where v is the vehicle speed.

The energy consumption during driving can be further calculated based on the driving distance and energy efficiency, as described below:

$$E_{pc} = \frac{d \cdot e}{\varepsilon} \tag{3}$$

where E_{pc} is the energy consumption of an EV, d is the distance, e is the energy consumption per unit distance, and ε is the energy efficiency.

2.3.3 SOC

The SOC reflects the ratio of the current battery capacity to the rated capacity of the electric vehicle, and can be calculated using the following formula:

$$SOC_i = \frac{E_i}{E_{bat}} \tag{4}$$

where E_i could be initial power storage, power consumption, remaining storage, and charging demand (denoted as E_{ori}, E_{pc}, E_{rem}, and E_{char}), corresponding to the initial, consumed, remaining, and chargeable SOCs of an EV (denoted as SOC_{ori}, SOC_{pc}, SOC_{rem}, and SOC_{char}).

2.3.4 Parking period

The parking duration is related to the arrival and departure time at the charging station. According to a field survey on transportation in Beijing [33], the departure time from the charging station follows a normal distribution (with a mean value of 7:45 and a standard deviation of 1 hour), and the arrival time at the charging station also follows a normal distribution (with a mean value of 19:00 and a standard deviation of 1.5 hours). From this information, the parking duration of users can be determined.

3 Two-stage operation optimization model

3.1 Day-ahead stage

In the day-ahead stage, the load curve and the output of wind and solar power are significantly mismatched. To promote the consumption of wind and solar power, DVPBDR is used to send price signals to guide users to charge their EVs in an orderly manner.

3.1.1 Virtual price model

The mechanism for electricity pricing in China is still incomplete, and the existing pricing system to some extent restricts the efficient utilization of power resources [33]. Therefore, it is difficult to truly reflect the market supply and demand situation, and it cannot cope with unexpected or new peaks in demand, which goes against the original intention of optimization.

Based on the theory of time-of-use pricing, assuming that the electricity pricing mechanism is

not constrained by actual policies and regulations, it can freely fluctuate with changes in load, with no limit to the range of fluctuations. This is defined as virtual price. The virtual price may exist beyond the controllable range of the actual market, and therefore, it is not used as an actual transaction price, but only as a price signal for management to guide users to orderly charging and to enhance the peak-shaving and valley-filling capabilities of EVs. In addition, static time-of-use pricing cannot adjust prices according to changes in load, which may cause a large number of price-sensitive users to shift their loads to fixed low-price time periods, thus resulting in "peak-valley inversion". On the contrary, virtual price is dynamically updated. Price signals are sent to each upcoming user, which can more accurately and meticulously reflect supply and demand relationships and provide differentiated charging strategies.

This paper introduces the concept of net load P_{net}, which refers to the total demand for electricity (excluding EVs about to be connected to charging piles) minus the wind and solar power generation. The purpose is to encourage users to charge their EVs during periods of high wind and solar power generation, while smoothing the load curve. The day is divided into 48 periods, each lasts 30 minutes, and the relationship between virtual price and load can be described as follows [33]:

$$P_{net,t} = P_{regular,t} + P_{ch,t/z} - P_{wp}(v(t)) - P_{pv}(t) \tag{5}$$

$$\gamma_{v,t}(z) = b_1 \cdot P_{net,t} + b_2 \cdot (P_{net,t} - P_t^{ref,1}) + b_3 \tag{6}$$

$$b_1 = \frac{\gamma_{ref,1}}{P_{c,t}^{ref,1}} \tag{7}$$

$$b_2 = \frac{\gamma_{ref,2}}{P_{c,t}^{ref,2}} \tag{8}$$

where $\gamma_{v,t}(z)$ is the virtual price of user z at time t, $P_{ch,t/z}$ is the charging load at time t when user z is about to charge, b_1, b_2 and b_3 are coefficients (b_3 is a constant), $P_{c,t}^{ref,1}$ and $P_{c,t}^{ref,2}$ respectively are the regular valley load and the peak-valley difference, $\gamma_{ref,1}$ and $\gamma_{ref,2}$ respectively are the regular valley price and the peak-valley price difference. The derivative of the above formula is $b_1 + b_2 > 0$, which indicates a positive correlation between current load level and virtual price. $\gamma_{v,t}(z) < b_3$ or $\gamma_{v,t}(z) < 0$ indicates the existence of wind and solar power curtailment, so this formula can reflect the consumption of wind and solar power.

3.1.2 Day-ahead optimization based on DVPBDR

Based on the virtual price, the concept of "virtual charging cost" is introduced as the optimization objective function in the day-ahead stage. Since the virtual price is determined based on the wind and solar power usage at each time step, a small amount of net load may indicate surplus

wind and solar power, resulting in a lower virtual price, while the opposite will result in a higher virtual price. Therefore, when the virtual charging cost reaches its minimum, the wind and solar power utilization is at its highest. The optimization objective is formulated as follows:

$$\min C_v = \sum_{z=1}^{Z} \sum_{t=1}^{48} [\gamma_{v,t}(z) \cdot P_{ch,t}(z)] \tag{9}$$

where C_v is the virtual charging cost, and z is the number of users.

3.2 Intraday stage

Due to the uncertainty of wind and solar power, the prediction results have certain deviations. In the intraday stage, NO, DGO and CA participate in the bi-layer Stackelberg game, to further adjust the charging plan, reduce the impact caused by wind and solar deviation, and enable all participants to obtain satisfactory benefits.

3.2.1 Strategic analysis and game formulation

The NO has the ability to increase the selling price of electricity in order to maximize its profits, but this would also raise the purchasing cost for the DGO. If the purchasing price exceeds the penalty for load shedding, the DGO may resort to cutting some load, which unfortunately may not be satisfactory for users.

In the process of energy trading, NO's price strategy will affect DGO's electricity purchase volume, and DGO's price strategy will affect CA's adjustment of charging load. Conversely, the adjusted charging load changes the peak-valley level of the overall load and the wind and solar power consumption, which may also cause changes in DGO's electricity purchase from NO, and NO will adjust the price accordingly. Participants interact and constantly adjust their strategies to coordinate their interests. In this process, each stakeholder is an independent individual, and their interests conflict to some extent. Moreover, decision-making is sequential. Therefore, Stackelberg game is applicable to address this problem [25]. This paper proposes a bi-layer Stackelberg game to solve the charging system problem with three participants. In this system, DGO serves as the intermediate level, following NO in the upper-layer game while leading CA in the lower-layer game. Based on this, the bi-layer game model can be formulated as follows:

$$G = < P; S; U > \tag{10}$$

where P is the participant set, S is the strategy set, U is the utility set. The participants in the bi-layer Stackelberg game model are the NO, DGO, and CA. Their strategy sets include the selling price of electricity for the NO, the power purchase and selling price for the DGO, and the charging demand for the CA. Utility functions for each player are described in Section 3.2.2 and will not be discussed in detail here. For the bi-layer Stackelberg game to obtain equilibrium solutions, the following constraints must be met:

$$\begin{cases} U_{gird}(\gamma_g^{op}, P_{gd}^{op}, \gamma_{mg}^{op}, P_{sd}^{op}) \geq U_{gird}(\gamma_g, P_{gd}^{op}, \gamma_{mg}^{op}, P_{sd}^{op}) \\ U_{mg}(\gamma_g^{op}, P_{gd}^{op}, \gamma_{mg}^{op}, P_{sd}^{op}) \geq U_{mg}(\gamma_g^{op}, P_{gd}, \gamma_{mg}, P_{sd}^{op}) \\ U_{user}(\gamma_g^{op}, P_{gd}^{op}, \gamma_{mg}^{op}, P_{sd}^{op}) \leq U_{user}(\gamma_g^{op}, P_{gd}^{op}, \gamma_{mg}^{op}, P_{sd}) \end{cases} \tag{11}$$

where γ_g^{op}, P_{gd}^{op}, γ_{mg}^{op}, and P_{sd}^{op} are the selling price equilibrium strategy of the NO, power

purchase equilibrium strategy of the DGO, selling price equilibrium strategy of the DGO, and charging equilibrium strategy of the CA, respectively. The above conditions indicate that the equilibrium strategies of all participants can lead to maximum utility for each participant. That is, when all participants reach their equilibrium strategies, no one can obtain more benefits by independently adjusting their strategies. When the equilibrium strategies are reached, no one will get more benefits by adjusting the strategy secretly.

3.2.2 Objectives and constraints of upper-layer game

The participants in the upper-layer game are the NO and the DGO, and the game information is shown in Figure 3.

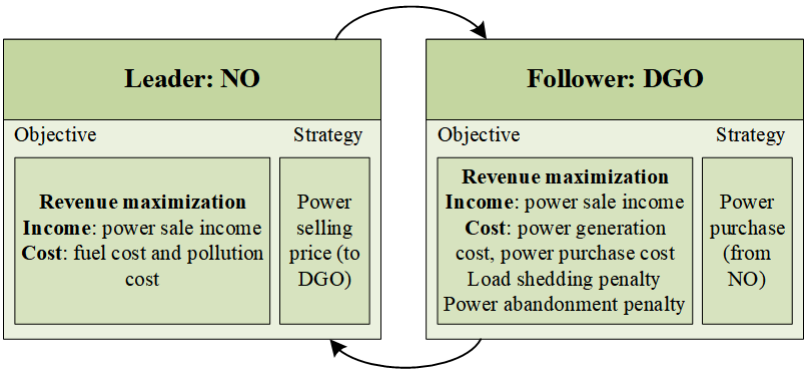

Figure 3 Upper-layer game information

In the upper-layer game, the NO maximizes its net income with the selling price as the strategic variable, while the DGO maximizes its net income with the purchased electricity as the strategic variable. The game is played by the NO changing the price and DGO adjusting the quantity of purchased electricity. After reaching a temporary equilibrium, DGO's purchased electricity quantity is passed down to the lower-layer game. The specific objective functions and constraints are as follows:

(1) Objectives

The NO's net income includes revenue from selling electricity, the cost of thermal power generation, and the cost of pollutant emissions, as follows:

$$\max U_{gird} = \sum_{t=1}^{48} (\gamma_{g,t} P_{gd,t} - C_{g,t} - C_{po,t}) \tag{12}$$

$$C_{g,t} = a_1 \cdot (P_{gd,t})^2 + a_2 \cdot P_{gd,t} + a_3 \tag{13}$$

$$C_{po,t} = \sum_{n=1}^{N} (\gamma_{po,n} \cdot \omega_n \cdot P_{gd,t}) \tag{14}$$

where U_{gird} is the revenue of NO, $\gamma_{g,t}$ is the selling price of NO, $P_{gd,t}$ is the purchased power of DGO, $C_{g,t}$ is the power generation cost, $C_{po,t}$ is the pollutant treatment cost, a_1, a_2 and a_3 are the parameters of thermal power generation, n is the kind of pollutant, $\gamma_{po,n}$ is the pollutant

treatment price, and ω_n is the emission factor.

The net income of the DGO is composed of revenue from selling electricity, the unit cost of wind and solar power generation, the cost of purchasing electricity from NO, the penalty for wind and solar curtailment, and the penalty for load shedding, which is detailed as follows:

$$\max U_{dg} = \sum_{t=1}^{48} (\gamma_{dg,t} P_{sd,t} - \gamma_{g,t} P_{gd,t} - C_{wpv,t} - \gamma_{qn,t} F_{qn,t} - \gamma_{pc,t} P_{pc,t}) \tag{15}$$

where U_{dg} is the revenue of DGO, $\gamma_{dg,t}$ is the selling price, $P_{sd,t}$ is the power sales, $C_{wpv,t}$ is the unit cost of wind and solar power generation, $\gamma_{qn,t}$ is the coefficient of power curtailment penalty, $F_{qn,t}$ is the energy curtailment, $\gamma_{pc,t}$ is the coefficient of load shedding penalty, $P_{pc,t}$ is the unsatisfied load.

(2) Constraints

1) Capacity constraint of distribution transformer

For safety reasons, the power output of the DGO must be within the maximum capacity range of the distribution transformer they are connected to in each time period, i.e.:

$$(P_{gd,t} = P_{sd,t} + P_{reg,t} - P_{wp}(v(t)) - P_{pv}(t)) < P_{MTF} \tag{16}$$

where $P_{reg,t}$ is the regular load at time *t*, and P_{MTF} is the maximum carrying capacity of distribution transformer.

2) Selling price constraint of NO

$$\gamma_g^{\min} \le \gamma_{g,t} \le \gamma_g^{\max} \tag{17}$$

where $\gamma_g^{\min}$ and $\gamma_g^{\max}$ are the lower and upper limits of NO's selling price.

3) Power purchase constraint

The reverse power transmission from DGO is not considered, so the power purchase is constrained as follows:

$$P_{gd,t} \ge 0 \tag{18}$$

3.2.3 Objectives and constraints of lower-layer game

The participants in the lower-layer game are the DGO and CA, and the game information is shown in Figure 4.

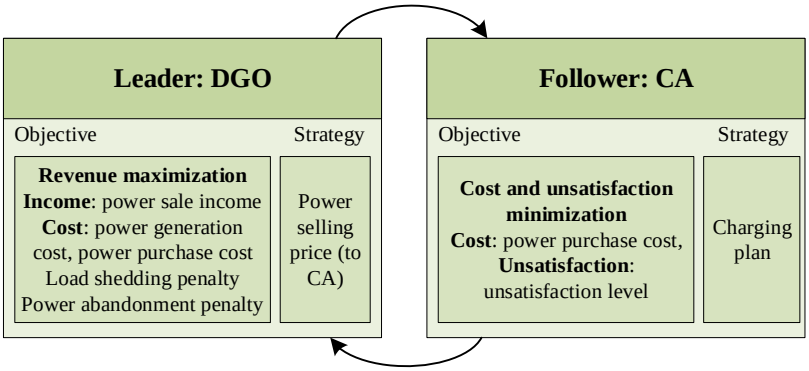

Figure 4 Lower-layer game information

In the lower-layer game, the DGO aims to maximize its net income, with the selling price being the strategy variable; while the CA's goal is to minimize the cost of charging and user dissatisfaction, with the charging plan as the strategy variable. The game is played by the DGO changing the selling price and CA adjusting the charging plan. Once equilibrium is achieved, the amount of load that cannot be met by DGO is passed on as the purchase demand to the upper layer. The objective functions and constraints are detailed as follows:

(1) Objectives

For DGO: See Equation 15;

For CA:

The benefit of the CA includes two aspects: minimizing the charging cost and minimizing the level of user dissatisfaction. The charging cost is as follows:

$$\min u_1 = \sum_{t=1}^{48} (\gamma_{dg,t} \cdot P_{sd,t}) \tag{19}$$

This paper adopts a reverse evaluation method of dissatisfaction to represent users' energy consumption experience. The user dissatisfaction model is constructed as follows [26]:

$$\min u_2 = \frac{1}{48} \sum_{t=1}^{48} \beta[-1 + \alpha^{\chi(1-\frac{P_{sd,t}}{P_{0,t}})}] \tag{20}$$

where α, β, and χ are the parameters ($\alpha, \chi > 1$ and $\beta > 0$), and $P_{0,t}$ is the initial load. $u_2 > 0$ indicates the dissatisfaction of users, while the dissatisfaction turns into satisfaction when $u_2 \le 0$. The ultimate form is shown below:

$$\min U_{user} = \lambda_1 u_1^{'} + \lambda_2 u_2^{'} \tag{21}$$

where λ_1 and λ_2 are the weights of the two objectives respectively, $u_1^{'}$ and $u_2^{'}$ are the dimensionless values of each objective after normalization.

(2) Constraints

1) Selling price constraint of DGO

$$\gamma_{mg}^{\min} \le \gamma_{mg,t} \le \gamma_{mg}^{\max} \tag{22}$$

where $\gamma_{mg}^{\min}$ and $\gamma_{mg}^{\max}$ are the lower and upper limits of DGO's selling price.

2) Wind and solar power output constraints

$$P_{wp}^{\min} \le P_{wp}(v(t)) \le P_{wp}^{\max} \tag{23}$$

where $P_{wp}^{\max}$ and $P_{wp}^{\min}$ are the maximum and minimum dispatchable outputs of wind generator.

$$P_{pv}^{\min} \le P_{pv}(t) \le P_{pv}^{\max} \tag{24}$$

where $P_{pv}^{\max}$ and $P_{pv}^{\min}$ are the maximum and minimum dispatchable outputs of photovoltaic generator.

3) Supply and demand balance

Power balance is constrained between supply and demand in each time period, i.e.,

$$D(t) = S(t) \tag{25}$$

$$D(t) = P_{ch,t} + P_{reg,t} \tag{26}$$

$$S(t) = P_{gd,t} + P_{wp}(v(t)) + P_{pv}(t)) + P_{gd,t} + D_{EVd,t} \tag{27}$$

where $D(t)$ is the demand at time *t*, and $S(t)$ is the supply at time *t*.

4) Safe storage constraint

The battery has bounds for safe storage to avoid damages from over-charging or low power, which is given by

$$E_{ra} \cdot \xi \le E_n \le E_{ra} \cdot \zeta \tag{28}$$

where E_n is the amount of stored electricity, E_{ra} is the rated power, ζ and ξ are the safe storage bounds.

5) Charging power constraint

The charging power of EVs cannot exceeds the rated bounds, i.e.,

$$P_{ch,t}^{\min} \le P_{ch,t} \le P_{ch,t}^{\max} \tag{29}$$

where $P_{ch,t}^{\min}$ and $P_{ch,t}^{\max}$ are the minimum and maximum charging powers.

6) Charging duration constraint

$$\begin{cases} t_{arr} \le t_c \le t_{dep} \\ T_c \le T_{dwell} \end{cases} \tag{30}$$

where t_c is the charging moment, T_c is the charging period, t_{arr} is the time when an EV arrives at the station, t_{dep} is the time when an EV departs from the station, and T_{dwell} is the dwelling period.

3.2.4 Bi-layer Stackelberg game process

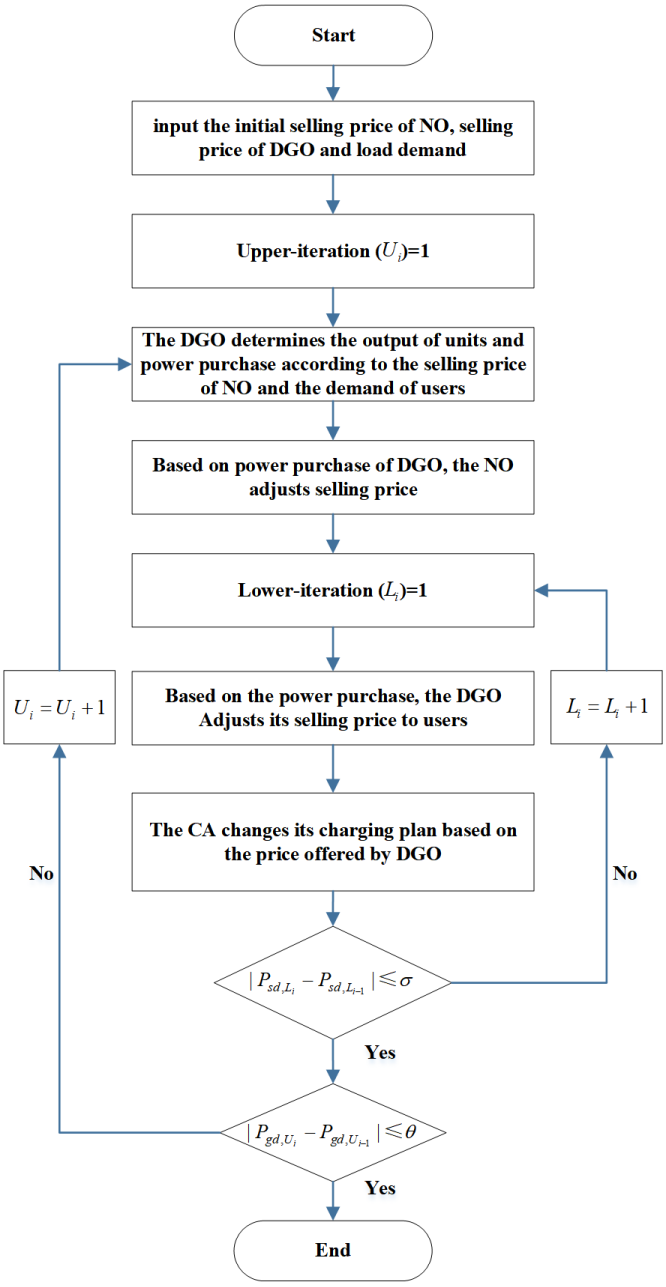

Figure 5 Process of bi-layer Stackelberg game

The process of the proposed bi-layer Stackelberg game is shown in Figure 5. The initial prices of NO and DGO and the charging demand are input. The upper-layer game begins with the DGO determining its output plan based on the initial charging demand and reporting the purchased electricity to the NO. The NO adjusts its selling price to maximize its net income according to the

purchase quantity declared by the DGO and transmits the price signal to the DGO. The DGO then adjusts its purchase quantity based on the price offered by the NO. In the lower-layer game, the DGO determines the selling price based on the current load level and purchased electricity, and transmits the price signal to the CA. Upon receiving the signal, the CA adjusts its charging plan and reports it back to the DGO. The game continues until equilibrium is reached.

4 Case analysis

4.1 Preparation

4.1.1 Case setup

As shown in Table 1:

- Case 1: basic scenario where no day-ahead scheduling is considered, and users charge their EVs disorderly.
- Case 2: day-ahead optimization is conducted based on the DVPBDR model to obtain a charging scheduling plan, which is then executed during the intraday stage.
- Case 3: day-ahead optimization using DVPBDR is conducted, and multi-participant multi-objective charging optimization is conducted during the intraday stage as described in [22].
- Case 4: day-ahead optimization using DVPBDR is conducted, and during the intraday stage, a bi-layer mixed game is employed based on the approach described in references [36, 40]. The DGO and CA form a new operational coalition and engage in non-cooperative gaming with the NO. The cooperative benefits are then allocated between the DGO and CA using the Shapley method, which is described in the Appendix.
- Case 5: day-ahead DVPBDR optimization is conducted, and during the intraday stage, a bi-layer mixed game is employed. Drawing inspiration from [36, 40], this case assumes that the NO owns wind and PV power generators (i.e., forming a new operational coalition with the DGO). The NO engages in a non-cooperative game with the CA, and the resulting income is allocated between the two business transactions of renewable supply and electricity purchase from the public grid using the Shapley method.
- Case 6: day-ahead DVPBDR optimization is carried out, and a bi-layer Stackelberg game is employed during the intraday stage to adjust to deviations in renewable energy output.

Table 1 Case setup

Case	Day-ahead: DVPBDR	Intraday: bi-layer game
1	×	×, disordered charge
2	√	×, scheduling based on the day-ahead plan
3	√	×, multi-objective optimization
4	√	√, bi-layer mixed game (upper: non-cooperation, lower:

		cooperation)
5	√	√, bi-layer mixed game (upper: cooperation, lower: non-cooperation)
6	√	√, bi-layer non-cooperative (Stackelberg) game

4.1.2 Basic data

Based on the charging model presented earlier, the travel and charging information of 200 EVs are generated. In addition, the rated capacity of an EV is set to be 82 kWh, the energy efficiency of driving is set to be 90%, and the charging efficiency is set to be 95%, following the work of Han et al. [41]. The disorderly charging load is shown in Figure 6. To make the simulation more realistic, we also introduce regular load [42]. The regular demands are also supplied by the DGO, and any shortfall is supplemented by the NO. The coefficients of user dissatisfaction, i.e., α, β, and χ, are set to be 3, 12, and 5, respectively.

The scenario generation-reduction method proposed in this paper is employed, and 1000 scenarios of wind power and photovoltaic power generation are generated and reduced to 20 scenarios each. The average value of the top 10 scenarios with the highest occurrence probability is taken to obtain the intraday wind and solar power generation curves, while the remaining scenarios are averaged to obtain the day-ahead wind and solar power generation curves, as shown in Figure 6. To ensure that the virtual prices are positive, b_3 is set to be 4.57. Price references of valleys and peaks and are set to be 0.7515 CNY/kWh and 1.3096 CNY/kWh respectively. The initial prices are set to be the same with the reference prices. The generation costs of wind and solar powers are set to be 0.25 CNY/kWh and 0.36 CNY/kWh, and the energy curtailment penalty is set to be 0.7515 CNY/kWh.

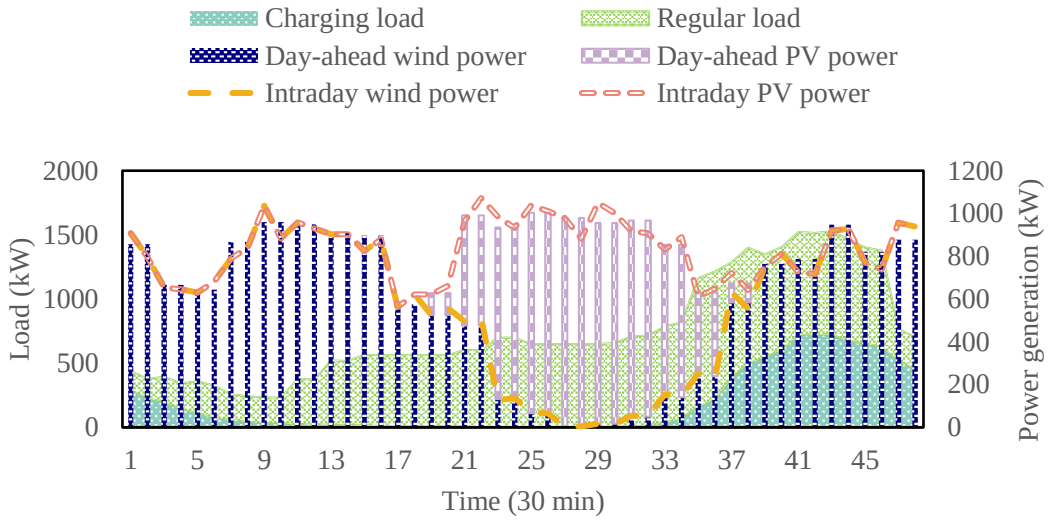

Figure 6 Wind and solar output and load

The initial price of NO is set to be 1.21 CNY/kWh, the fuel cost coefficients are set to be

$0.133*10^{-6}$, $126.5*10^{-3}$ and 0, gas emission control cost and emission coefficient are shown in Table 2 [43].

Table 2 Gas emission control cost and emission coefficient

Type of pollutant	Control expense (CNY/kg)	Emission coefficient (g/kWh)
CO_2	0.210	889.0
SO_2	14.842	1.8
NO_x	62.964	1.6

4.2 Results

4.2.1 Case 1

Renewable output and load during the intraday period of Case 1 are shown in Figure 8, and the scheduling results are presented in Table 3.

Table 3 Scheduling results of Case 1

Case	Net income of the NO (CNY)	Energy curtailment (kWh)	Net income of the DGO (CNY)	Charging cost of the CA (CNY)
Case 1	2938.86	5862.30	5066.34	5222.37

Based on Figure 8 and Table 3, it is evident that the majority of charging load was concentrated during the peak hours of regular load. This is mainly due to users starting to charge their vehicles immediately after returning home from work, coinciding with the beginning of peak hours of regular load. Moreover, users charged their vehicles independently and all concentrated on charging during a specific time period, resulting in unfavorable situations of peak load superposition. Additionally, the high output periods of wind and solar power were roughly concentrated in time intervals 1-17 and 23-34, corresponding to the valleys and flats of load. This resulted in a significant amount of abandoned wind and solar energy (totaling up to 5862.30 kWh of waste energy). Due to the addition of charging load, the DGO output was insufficient to meet the demand, resulting in the simultaneous phenomenon of "abandoned energy and power shortage" and severe supply-demand imbalances that required purchasing electricity from the NO. There was significant room for optimization during the night when there was a long parking time, and a large number of time intervals were vacant.

4.2.2 Case 2

Starting from Case 2, day-ahead DVPBDR optimization is introduced. The analysis is conducted in three parts: peak-shaving and valley-filling effect, changes in period division, and the optimized results of Case 2.

(1) The effect of DVPBDR on peak regulation

To minimize the virtual charging cost and evaluate the peak-shaving ability of the DVPBDR, two optimization directions are employed to guide EVs charging and compare their effectiveness. One direction considers the peak shaving of net load with wind and solar power consumption, while the other considers only load demand. The distribution of the total load after optimization is shown in Figure 7, and the optimization results are presented in Table 4.

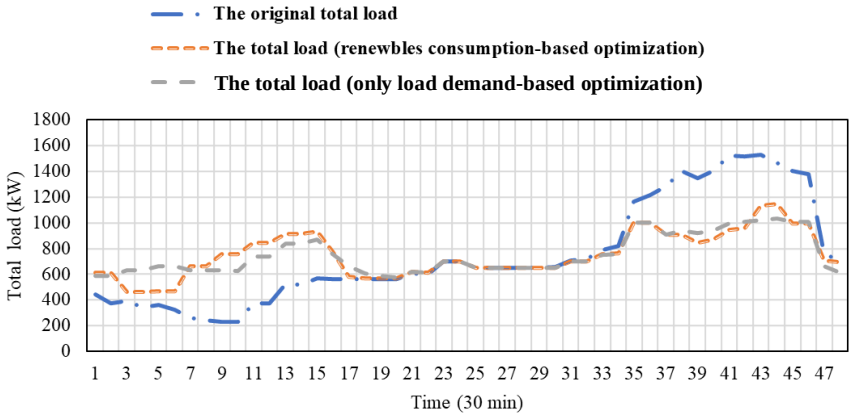

Figure 7 Total load distribution

Table 4 Optimization results of Case 2

Optimization direction	Virtual charging cost (CNY)	Day-ahead energy curtailment (kWh)	Peak-valley difference (kW)	Standard deviation of load fluctuation (kW)	Standard deviation of net load fluctuation (kW)
Disordered charge	/	5835.20	1294.74	323.03	362.11
Load demand-based	54537.39	3496.08	751.24	129.19	180.66
Renewables consumption -based	15798.15	3398.48	751.24	144.45	168.38

From Figure 7 and Table 4, it is evident that the load curve became significantly smoother after the DVPBDR optimization. Some users shifted their charging loads from peak periods to valley periods. Compared to disordered charge, the peak-valley difference decreased by 51.87%. As the optimization directions differ, the optimized curves showed different trends: the curve considering net load with wind and solar power consumption fluctuated similarly to wind and solar output during the user's charging periods, while the other optimization curve fluctuated similarly to the regular base load. Due to slight deviations in the optimization results from different directions, decision-makers can choose different optimization directions according to their specific decision-making needs. The main objective in the day-ahead stage was to reduce the curtailment of wind and solar power. The optimization based on renewables consumption consumed more renewable energy and had a lower “cost”. As a result, it was the chosen optimization approach in this paper.

To compare changes in the charging characteristics of five charging users randomly selected with their IDs as 64, 116, 119, 142, and 89, we analyzed their charging profiles before and after implementing an orderly charging strategy. As shown in Figure 8, the charging profiles of the users are disordered. In contrast, Figure 9 displays the charging profiles of the same users after applying

the ordered strategy, which optimized the virtual electricity price and scheduled charging sessions to occur at the lowest possible cost. During the orderly charging process, users adopted an intermittent charging pattern to reduce costs, in contrast to the continuous charging pattern adopted during the disordered charging process. Furthermore, users 116 and 119 followed the same charging trajectory during the disordered charging process, but due to the difference in their access time, their charging trajectories were slightly different after implementing the orderly charging strategy. This highlights the personalized and time-differentiated nature of the DVPBDR optimization strategy.

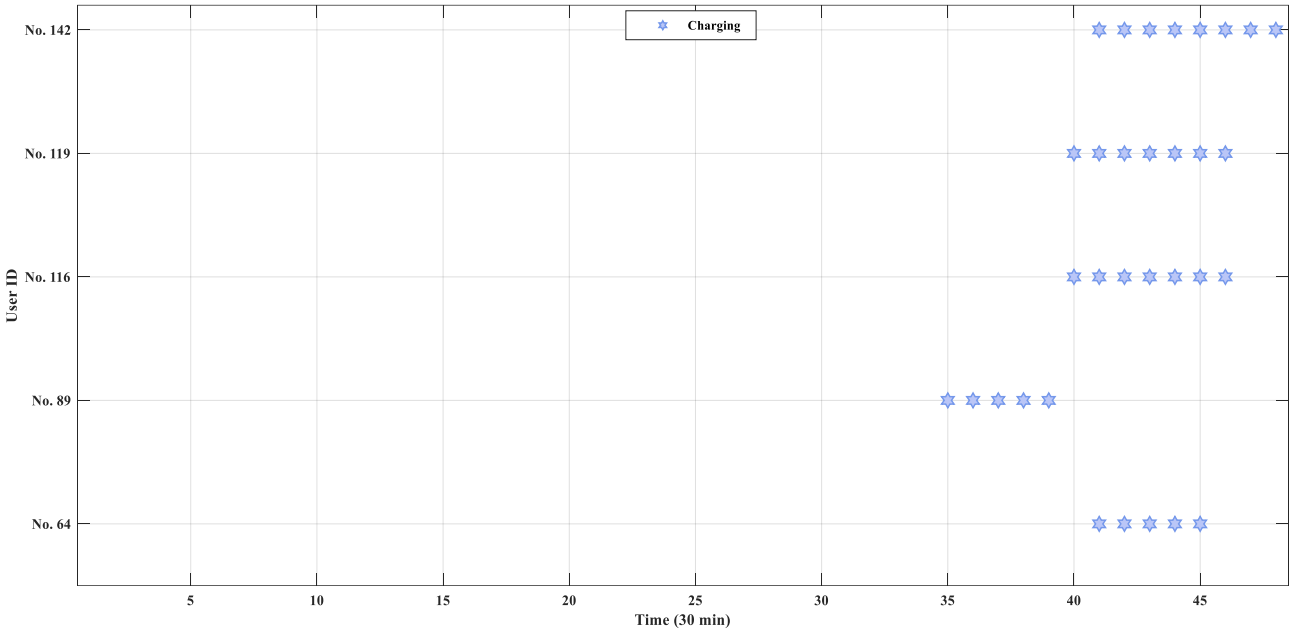

Figure 8 Time trajectory of disordered charging for individuals

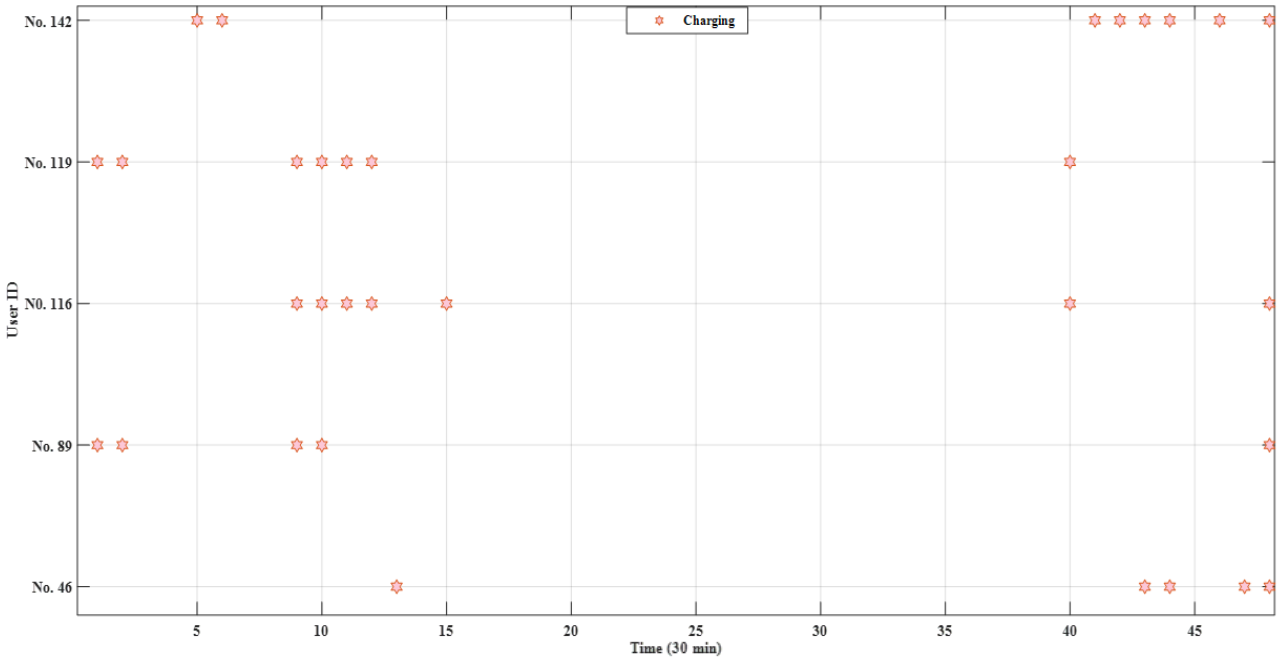

Figure 9 Time trajectory of optimized charging for individuals

(2) Period divisions (See Figure 10)

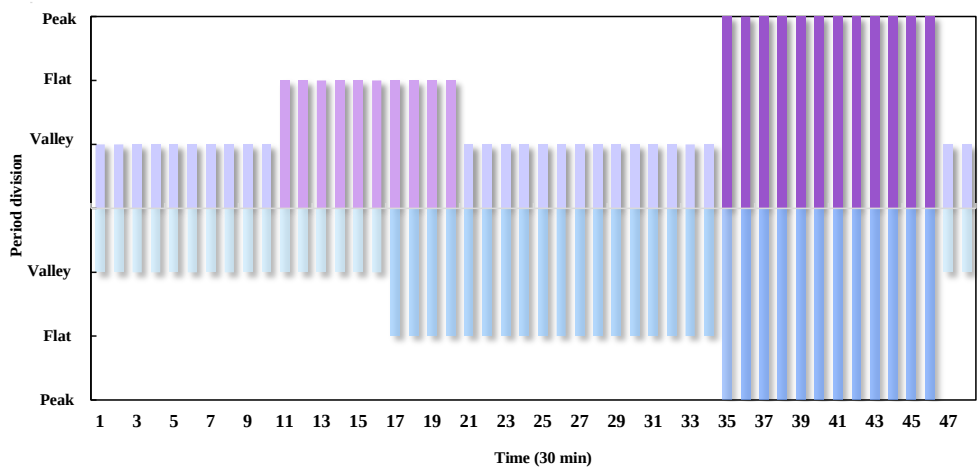

Figure 10 Changes of period divisions

According to Figure 10, the period changes were concentrated from 11 to 34. Users were encouraged to charge their charging demands in accordance with the fluctuations in wind and solar power output. Some demands in peak periods were shifted to the original valley periods 11-16, forming a "small peak". However, the main purpose of this strategy was to absorb excess wind and solar power without adding pressure to the distribution network, so they eventually clustered into flat periods. Due to load changes, the distance between the load at each time and the cluster center changed, leading to the original flat periods 21-34 being reclassified as valley periods. The renewable output in the original peak load periods could not fully meet load demands and required support from the NO, so they remained classified as peak periods after reclassification. The DGO still experienced abandoned energy in the remaining valley periods, and therefore they were still classified as valley periods.

(3) Scheduling results

Table 5 Scheduling results for Case 2

(Note: "Hypothetical dissatisfaction" refers to the dissatisfaction that arises when the load cannot be met by the originally planned "green electricity" due to deviations in wind and solar power. It is calculated using Equation 20)

Case	Net income of the NO (CNY)	Net income of the DGO (CNY)	Charging cost of the CA (CNY)	Dissatisfaction	“Hypothetical dissatisfaction”
Case 2	1103.38	8366.16	3842.13	0	63.32

The results of Case 2 are presented in Table 5. The day-ahead charging plan was executed in the intraday stage, so the charging dissatisfaction was 0. The charging plan was determined based on the trend of day-ahead forecast power output. However, due to the output uncertainty, there was a certain deviation between the actual and predicted outputs. When the actual output was less than the predicted output, the CA did not adjust the charging plan, causing some loads to be unable to be satisfied as planned, resulting in "hypothetical dissatisfaction" (with a value of 63.32, and this part of the load is finally satisfied by the NO). In addition, wind and solar power can meet most of the

load demands, so the DGO gained a large profit of 8366.16 CNY. Only a small portion of the demand was still supported by the NO, who had a net profit of 1103.38 CNY.

4.2.3 Case 3

The prices of the NO and DGO, charging load are shown in Figure 11, and the operation results are shown in Table 6.

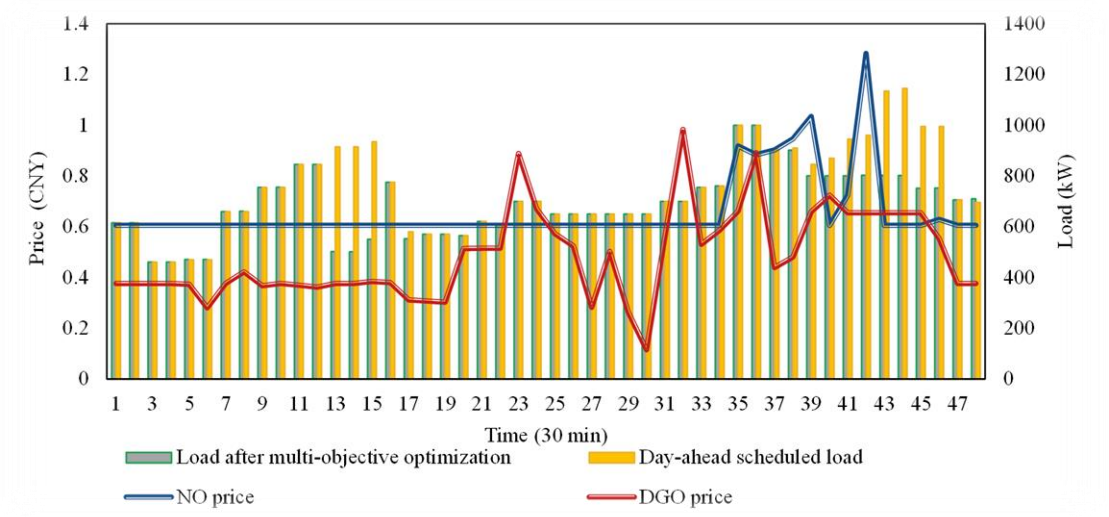

Figure 11 Prices of the NO and DGO and charging load

Table 6 Scheduling results of Case 3

(Note: "All-day charging dissatisfaction" refers to the dissatisfaction caused by the change in the total demands due to load reduction.)

Case	Net income of the NO (CNY)	Net income of the DGO (CNY)	Charging cost of the CA (CNY)	Dissatisfaction (Compared to Case 2)	All-day charging dissatisfaction
Case 3	988.34	6769.53	2313.12	790.35	55.07

As shown in Figure 11 and Table 6, the selling price of the DGO fluctuated mainly during non-peak hours (19-47), while the selling price of the NO mainly changed during the periods of 34-43 when the load was at peak. At this time, wind and solar power was not sufficient to meet the high demand, so the NO provided additional power supply. Although the load decreased significantly during the periods of 39-45 and 13-17, there was no obvious period of load increase. This is due to the goal conflict in the multi-objective joint optimization, which ultimately led to concessions by the CA, resulting in a large amount of load reduction and an all-day charging dissatisfaction of 55.07.

4.2.4 Case 4

In this case, the DGO and the CA form an alliance to engage in the non-cooperative game with the NO. The alliance's strategy was to negotiate the purchasing quantity of electricity from the NO. After forming the alliance, the CA adjusted its charging strategy to assist the DGO in purchasing electricity at a lower price. After the non-cooperative game ends, the cost savings from purchasing electricity are allocated using the Shapley value method, and the DGO returns the savings to users in the form of discounted prices. The optimized price of the NO, power purchase of the alliance,

and the load curve are shown in Figure 12. The operating results are shown in Table 7.

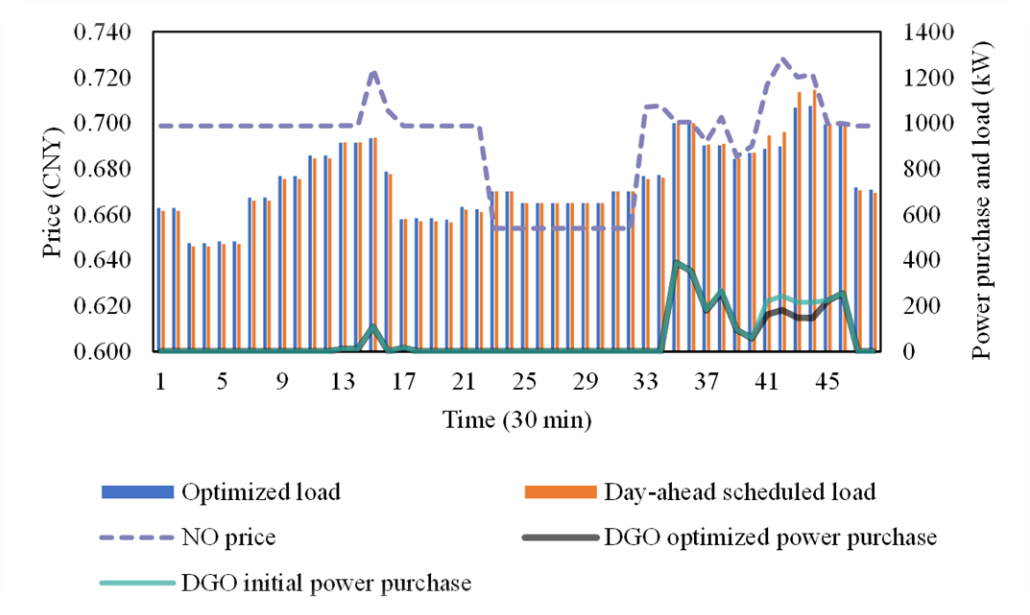

Figure 12 Optimized NO price, power purchase of the NO and CA, load changes

Table 7 Scheduling results of Case 5

Case	Net income of the NO (CNY)	Net income of the DGO (CNY)	Charging cost of the CA (CNY)	Dissatisfaction (Compared to Case 2)	All-day charging dissatisfaction
Case 4	1255.51	7993.10	3454.54	34.45	0

As shown in Figure 12 and Table 7, the price fluctuations of NO were consistent with the amount of electricity purchased by the alliance. The NO offered lower prices during periods when the alliance had no purchasing intentions, but increased prices once the alliance expressed interest in purchasing. The alliance attempted to reduce its electricity purchase demands during high-price periods by shifting its load. In the end, the alliance saved approximately 646.04 CNY in costs, with the contribution of the DGO and the CA being roughly equal at 1:1. As a result, the DGO returned half of the cooperative benefits to users in the form of price discounts. There was no load reduction throughout the entire process, so the all-day charging dissatisfaction was 0, but the load transfer resulted in a dissatisfaction of 34.45.

4.2.5 Case 5

In this case, the NO owns distributed energy resources, so only one pricing game is needed to determine the selling price to the CA. The CA's game strategy is still the charging load curve. After the game, the NO's selling price and charging demand are shown in Figure 13 and the optimization results are shown in Table 8.

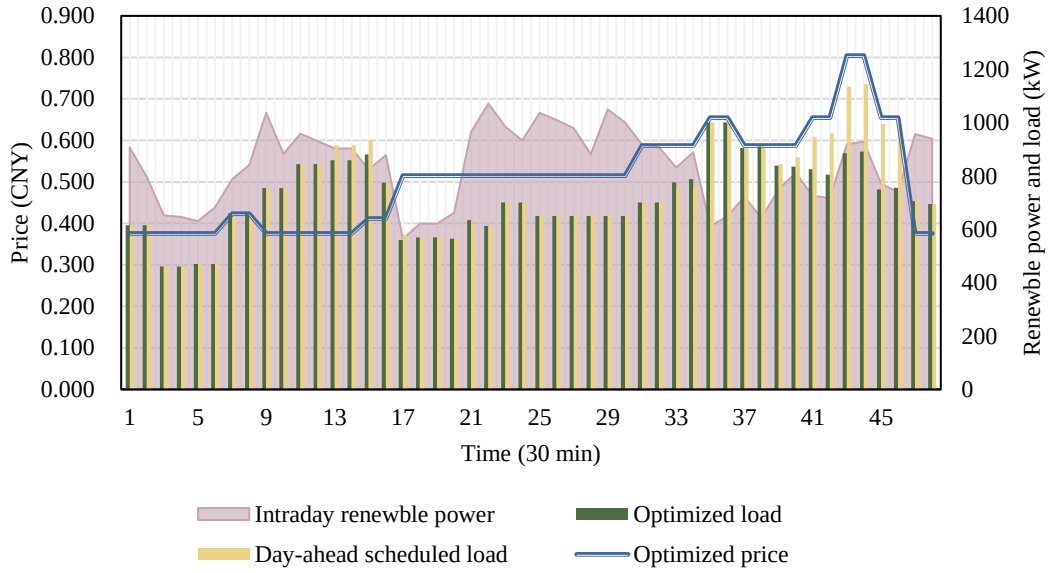

Figure 13 NO's selling price and charging load changes

Table 8 Scheduling results of Case 5

Case	Net income of the NO (CNY)	Net income of the DGO (CNY)	Charging cost of the CA (CNY)	Dissatisfaction (Compared to Case 2)	All-day charging dissatisfaction
Case 5	1371.95	8635.69	3935.42	190.69	0

As shown in Figure 13 and Table 8, the peak periods of 35-46 remains high-priced, and it is because the load in the periods were still high, and the CA was encouraged to shift it to valley hours of 1-12. During the periods of 17-34, there was still a large amount of abandoned energy because EV users were traveling at that time and cannot participate in dispatch. The change in electricity price during these periods cannot cause any leading effect, so the electricity price remained relatively stable. The alliance gained a net income of 10007.65 CNY. Based on the contributions of the NO and DGO (about 1:6.29), the NO final net income was 1371.95 CNY, and the DGO's was 8635.69 CNY. Due to non-compliance with the day-ahead scheduling plan, some users' charging plans were adjusted, resulting in dissatisfaction of about 190.69. However, only the charging load transfer happened instead of load cutting, and the all-day charging dissatisfaction was zero.

4.2.6 Case 6

The price changes and load changes are shown in Figure 14.

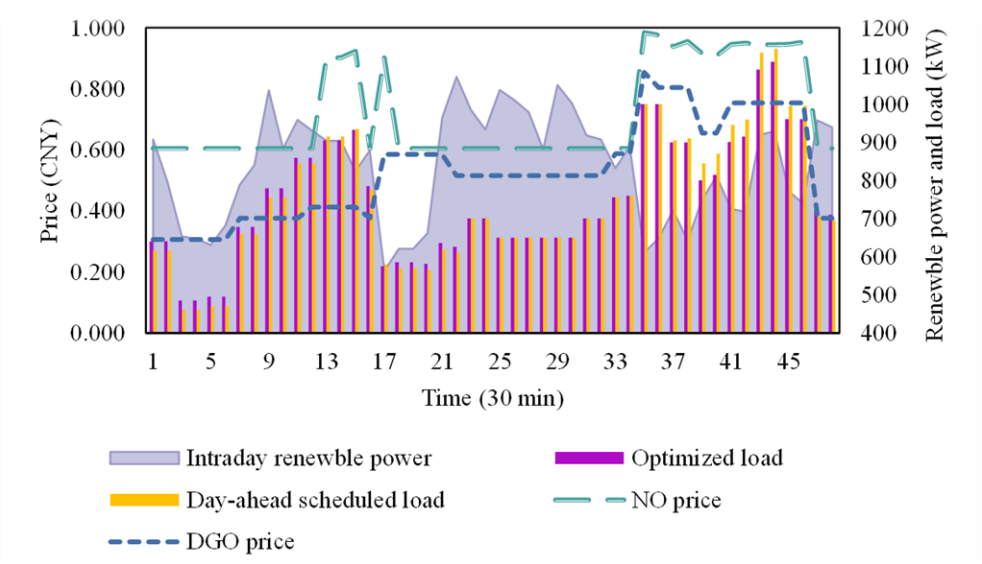

Figure 14 Price changes and load changes

Table 9 Scheduling results of Case 6

Case	Net income of the NO (CNY)	Net income of the DGO (CNY)	Charging cost of the CA (CNY)	Dissatisfaction (Compared to Case 2)	All-day charging dissatisfaction
Case 6	1830.06	9206.72	3808.29	202.21	0

As shown in Figure 14 and Table 9, similar to Case 4, the DGO guided some charging demand to the high power generation periods via low price strategy. The NO significantly raised its selling price due to load shift, resulting in a net profit of 1830.06 CNY. The DGO adopted a pricing strategy similar to that of the NO during the peak periods, while tending to price based on the trend of the load during the valley periods. Ultimately, the DGO gained a net profit of 9206.72 CNY. In the independent non-cooperative mode, each player ensured its own maximum benefits and did not compromise due to conflicting goals, especially the CA. There was no load reduction and only a dissatisfaction of 202.21 caused by load transfer.

4.3 Result comparison

In section 4.3.1, we introduce Case 7 to compare with the DVPBDR optimization and verify the superiority of the proposed approach in this paper. Sections 4.3.2-4.3.5 compare the intraday results in the cases, based on different evaluation dimensions. In section 4.3.6, weights are assigned to different evaluation indexes to compare the comprehensive optimization benefits and verify the effectiveness and superiority of the proposed bi-layer Stackelberg game.

4.3.1 Superiority analysis of the DVPBDR model

We set up Case 7 to verify the superiority of the proposed DVPBDR model. In Case 7, the virtual price is treated as the actual transaction price, with b_3 set to be 0 in Equation (6), and the actual transaction price is constrained between [0, 1.3096]. When the calculation result of Equation

(6) is negative, the transaction price is set to be 0, and when it exceeds 1.3096, the transaction price is set to be 1.3096 CNY. The total load curve is shown in Figure 15, and the results of abandoned energy, peak-valley difference, and net load fluctuation are shown in Table 10.

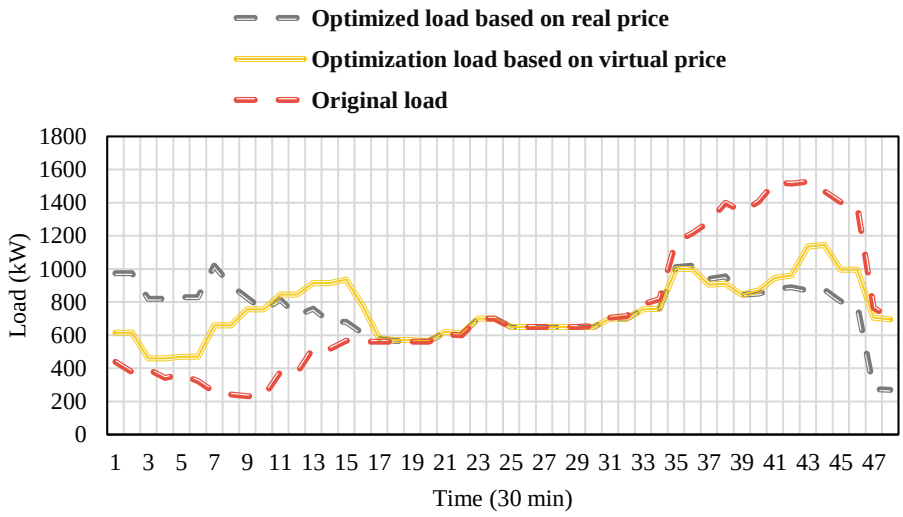

Figure 15 Day-ahead load changes based on actual transaction price and virtual price

Table 10 Day-ahead optimized results based on actual transaction price and virtual price

Optimization approach	Energy curtailment (kWh)	Peak-valley difference (kW)	Net load fluctuation (kW)
Based on actual transaction price	3541.35	750	191.44
Based on virtual price	3398.48	685	168.38

As shown in Figure 15 and Table 10, although the load curve optimized based on actual price can transfer the charging demand from peak periods 35-46 to off-peak periods 1-15, the resulting curve exhibited a significant "peak-valley inversion" and a new peak emerged. The peak-valley difference increased by 65 kW and the net load fluctuation increased by 23.06 kW, compared to the curve optimized based on virtual price.

In terms of renewable energy consumption, due to the constraint of actual transaction price, the DGO could only set the price at the extreme value when the electricity price exceeded the limit. In this case, the CA could not determine which sub-periods have further optimization space, and the incentive power of electricity price was significantly weakened. As a result, the effect of wind and solar energy consumption was not as good as the optimization results based on virtual price (the abandoned energy increased by 142.87 kWh compared to the virtual price-based case).

4.3.2 Comparison of dissatisfaction

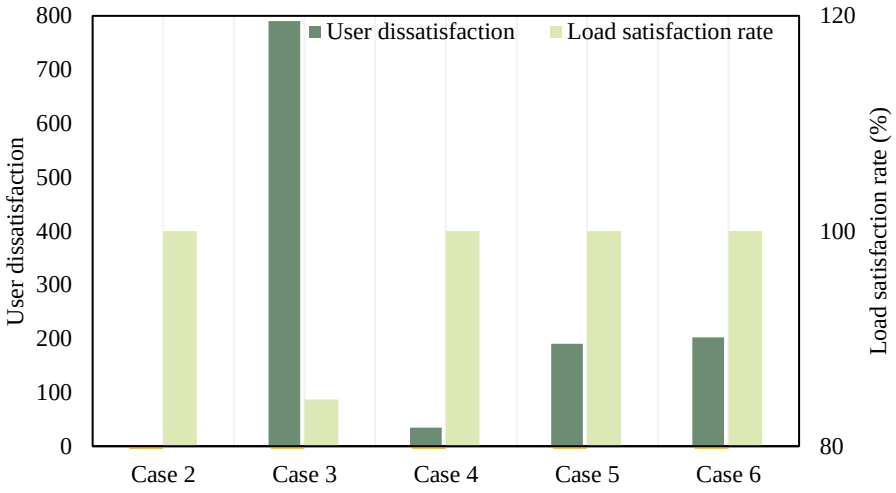

Figure 16 Dissatisfaction and load cutting in different cases

As illustrated in Figure 16, in Case 2, the intraday charging schedule was executed as planned, resulting in zero charging dissatisfaction. However, in the subsequent cases, the charging plan was further adjusted based on wind and solar deviations, leading to varying degrees of charging dissatisfaction. Case 3 showed the highest dissatisfaction as it involved both load transfer and load reduction. Cases 5 and 6 exhibited similar dissatisfaction levels of around 200, as both the bi-layer mixed game: NO-DGO alliance and the bi-layer Stackelberg game focused on charging demand as one of the non-cooperative game strategies. Case 4 had the lowest dissatisfaction level of 34.45, even though it was also a bi-layer game. This was because in Cases 5 and 6, the charging demand in the periods of 37-39 was fully transferred (the impact of full-load transfer on dissatisfaction calculation is significant). In contrast, in Case 4, the charging load in those periods was only partially transferred constrained by the cooperative relationship between the DGO and CA, as full transfer would increase CA's relative contribution and the benefits of CA, thereby reducing the cooperative benefits of DGO. Furthermore, Case 3 involved a significant amount of load reduction, resulting in an 84.34% load satisfaction rate, while in other scenarios, only load transfer occurred, leading to a 100% load satisfaction rate.

4.3.3 Comparison of load fluctuation

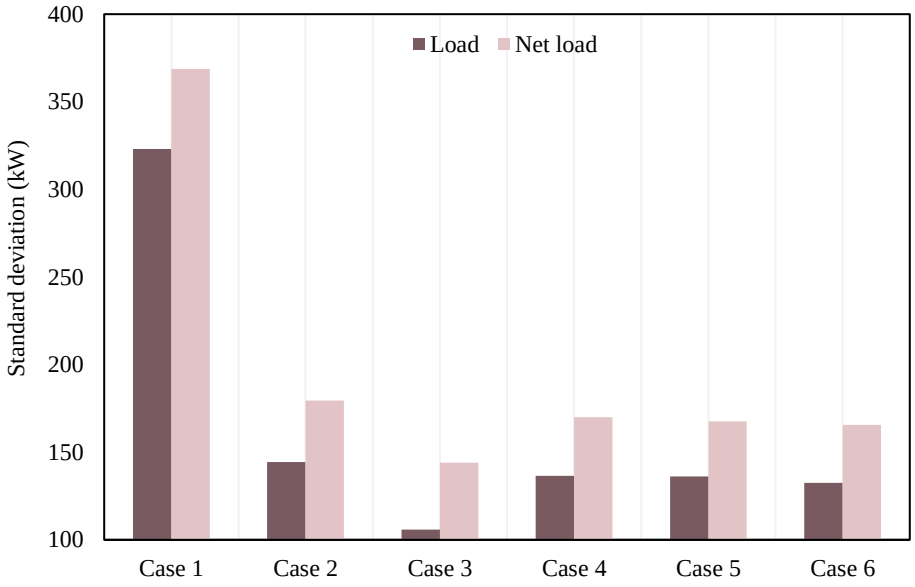

Figure 17 Load fluctuation in different cases

As shown in Figure 17, in the disordered charge case, charging demand often started as soon as the users arrived home, which coincided with the peaks for other regular usage, exacerbating the load pressure in peak time and resulting in greater load fluctuations. However, in Case 2 and subsequent cases, the day-ahead optimization with the DVPBDR resulted in an overall load distribution that trended towards wind and solar power generation, significantly flattening the load curve. The load fluctuation and net load fluctuation decreased by at least 55.28% and 51.33%, respectively. Additionally, Case 3 had the lowest load fluctuations, primarily due to the significant reduction of charging loads during peak periods. However, this had a negative impact on user satisfaction. Moreover, the load fluctuations in Cases 4 to 6 gradually decreased, with Case 6 having the lowest load fluctuation. This was because of the relationship between the fluctuation level and the amount of load transfer. According to the results in Section 4.3.2, Case 6 had the highest charging dissatisfaction and the largest load transfer amount, so the load curve in this case was more stable.

4.3.4 Comparison of renewable energy usage

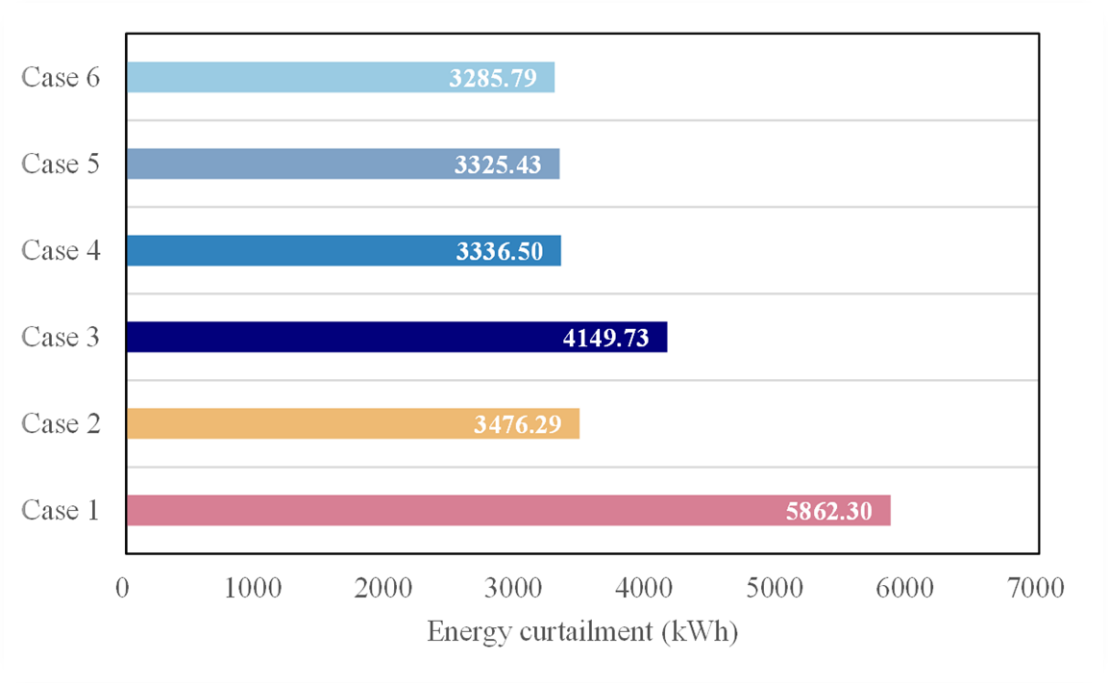

Figure 18 Energy curtailment in different cases

As shown in Figure 18, in the disordered charge case, a large amount of wind and solar energy was wasted due to the mismatch between their output and the load demand. With the implementation of the day-ahead DVPBDR, the amount of curtailed energy in Case 2 was significantly reduced by about 40.70%. In Case 3, the curtailed energy increased by 19.37% (compared to Case 2) due to excessive load shedding, and it led to a reverse increase in wind and solar usage. In the three bilayer game cases, there was generally a negative correlation between curtailed energy and load transfer. Compared to Case 2, the curtailed energy was reduced by 4.02%, 4.34%, and 5.48% in the three cases, respectively.

4.3.5 Comparison of economic benefits

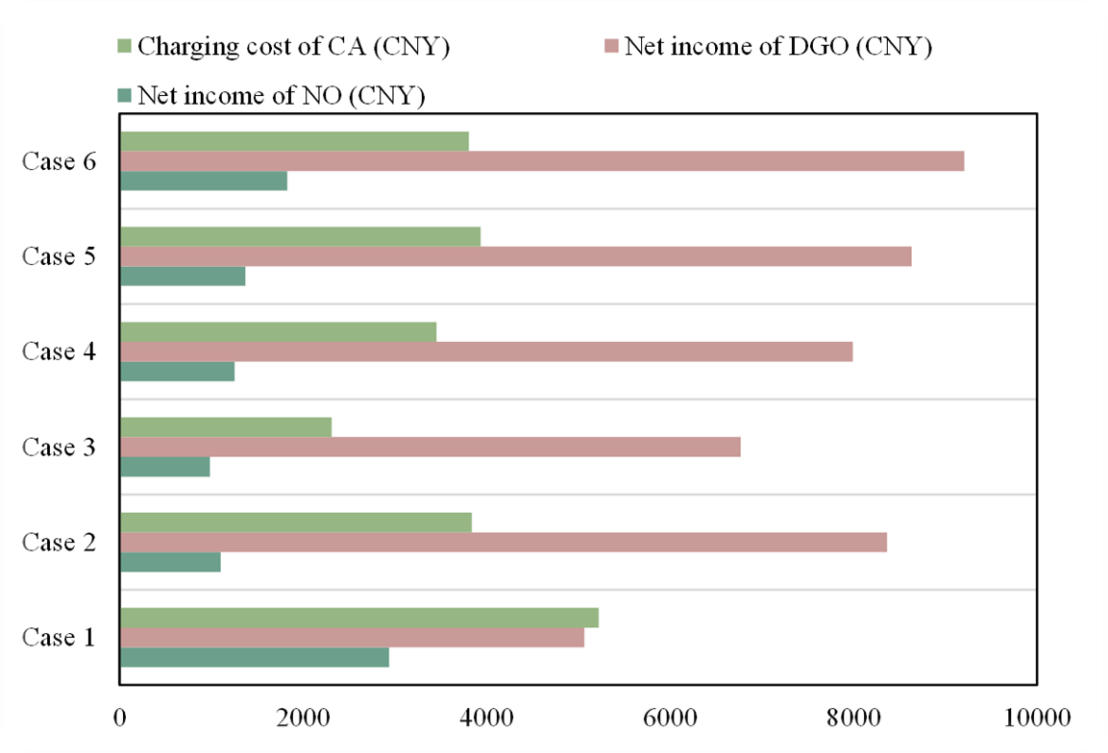

Figure 19 Economic benefits in different cases

As shown in Figure 19, for the NO, the net income ranking was, from highest to lowest, Case 1, Case 6, Case 5, Case 4, Case 2, and Case 3. For the DGO, the net income ranked, from highest to lowest, Case 6, Case 5, Case 2, Case 4, Case 3, and Case 1. For the CA, the charging cost ranking was, from lowest to highest, Case 3, Case 4, Case 6, Case 2, Case 5, and Case 1.

In the disordered charge case (Case 1), a significant mismatch between the demand and wind/solar power output led to a substantial amount of abandoned energy by the DGO (who also had to pay high purchasing costs), and it resulted in poor profitability. The CA also incurred high charging costs. Consequently, the NO provided a large amount of electricity to support the system and gained high profits. In contrast, Case 2 involved DGO optimizing charging demand with the day-ahead DVPBDR, which guided CA to adjust the charging plan based on the day-ahead wind and solar power output. Therefore, more wind and solar power was absorbed. This resulted in a reduction in DGO's penalty for abandoning energy, decreased DGO's purchasing costs, and allowed the CA to benefit from lower charging prices. Although wind and solar power output prediction errors occurred, the impact was smaller than the benefit increase. Consequently, DGO's net profit increased by 65.13%, CA's charging costs decreased by 26.43%, and yet NO’s output decreased and so did its net profit (about a 62.46% decrease).

In the multi-participant joint optimization case (Case 3), although it seems that the CA had the lowest charging cost, this was not actually because of the cost savings brought about by load shifting, but rather due to the conflicts in objectives resulting in benefit crowding out. Ultimately, the CA made a compromise and reduced load, which resulted in a poor satisfaction of users. Due to the reduction in load demand, the profits of the NO and DGO in this case were unsatisfactory.

In the bi-layer mixed game optimization (Cases 4 and 5), the DGO was the key player in forming the alliances. Through cooperation with the NO, the net profit of NO increased by 24.34% compared to Case 2, and the net profit of DGO increased by 3.22%. Although the increase in DGO's profit was not significant, it greatly improved the benefits of NO. However, for the alliance with the CA, which no longer considered the price impact of DGO on CA, the CA became the main force of the alliance, and its contribution to the alliance became more prominent, resulting in the distribution of a portion of DGO's profits, which had a significant negative impact on the DGO (its net profits decreased by 4.46% compared to Scenario 2). However, CA's charging cost was reduced by 10.09%. In the bi-layer mixed game, the cooperation between the DGO and the NO was more likely to achieve a relatively win-win.

In the bi-layer Stackelberg game optimization (Case 6), all operators were independent and pursued self-interest as their ultimate goal throughout the operation, without taking into account the interests of others. Therefore, they have gained more significant benefits in the game. Compared with other cases, the net incomes of NO and DGO increased by 85.17% and 36.00% at most, respectively, and the CA's charging cost decreased by 37.90% at most.

4.3.6 Comprehensive comparison

Due to the existence of multiple parties with multiple conflicting objectives, it is impossible to directly determine which case produces the best results. Therefore, we introduce the evaluation indicators from the perspectives of economic benefits, energy utilization, load stability, and user charging experience, as shown in Table 11. We use a comprehensive evaluation method [44] to obtain the final scores for each case. As shown in Figure 20, the final score for the bi-layer Stackelberg game case was the highest at 30.09%. Generally, compared with multi-participant joint optimization and bi-layer mixed game, the bi-layer Stackelberg game has superiority for the proposed charging system in this paper, which is more conducive to improving the multi-dimensional benefits of the system under multi-operator participation. The approach can positively incentivize the forementioned entities to participate in optimization and provide more favorable operational strategy references for them.

Table 11 Evaluation indexes and weights

Primary index	Weight	Secondary index	Index attribute	Weight
Economic benefit	3/4	Net income of NO	Positive	1/3
		Net income of DGO	Positive	1/3
		Charging cost of CA	Negative	1/3
Load stability	1/20	Net load fluctuation	Negative	1
Energy utilization	1/10	Energy curtailment	Negative	1
Charging experience	1/10	Charging dissatisfaction	Negative	3/4
		Load cutting	Negative	1/4

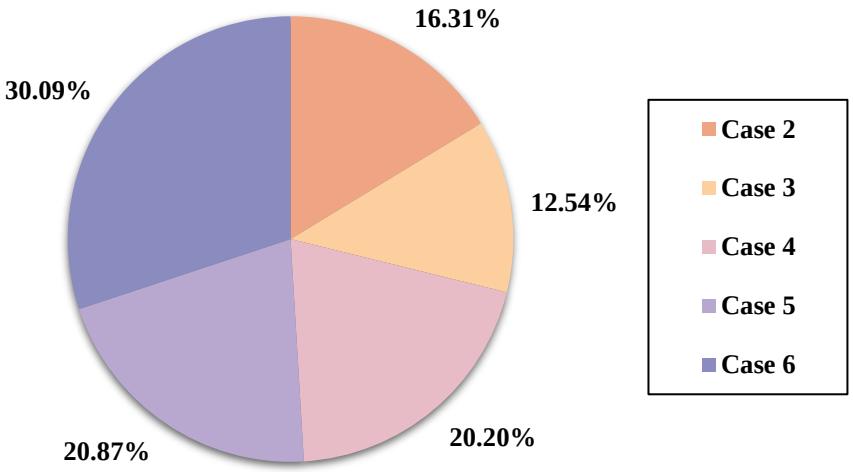

Figure 20 Comprehensive evaluation results of different cases

5 Conclusions

This paper proposed a charging system involving a NO, a DGO, and a CA in the context of non-cooperation among players. A two-stage charging optimization model considering the uncertainty of wind and solar power was constructed: In the first stage, a DVPBDR model is proposed to pre-optimize the charging load, in order to match the load demand with wind and solar power output as much as possible. Considering the generation deviation of wind and solar power, a deviation adjustment strategy based on a bi-layer Stackelberg game model was established in the second stage. The upper-layer game revolved around the pricing strategy of the NO and the power purchase strategy of the DGO, while the lower-layer game revolved around the selling price strategy of the DGO and the charging demand adjustment strategy of the CA. Case analysis shows that:

(1) the DVPBDR model can effectively break free from the constraints of the actual electricity pricing mechanism, more realistically reflect the guiding effect of electricity pricing changes on load demand, and improve the incentive ability of electricity pricing. By exchanging concepts, linking net load with clean energy consumption, the ordered charging program not only has the effect of peak regulation, but also reduces the waste of wind and solar power. Ultimately, the DVPBDR reduces wasted energy by 41.76% and reduces net load fluctuation by 53.50%.

(2) due to the conflicting interests among the participants, some of them chooses to concede during the optimization process under complete cooperation, which does not lead to the optimal outcome and resulted in suboptimal performance. On the contrary, in cases with non-cooperative games (either bi-layer mixed game or bi-layer Stackelberg game), the conflict among participants is weakened, and the non-cooperative participants reach their optimal outcomes through continuous information exchange and strategy adjustment, which also leads to the overall optimal performance of the system. Generally, the non-cooperative cases outperform the fully cooperative case with at least a 61.08% increase in comprehensive performance.

(3) In terms of partner selection, in the case of cooperation with CA, the CA makes a larger contribution to the alliance than the DGO, and therefore “diverts” a share of the revenue from the DGO. However, cooperation between the DGO and NO can promote an increase in revenue for the latter. As a result, the comprehensive benefits of the bi-layer mixed game with cooperation between

DGO and NO are 3.32% higher than that with cooperation between DGO and CA. Therefore, the cooperation of DGO with NO is more likely to achieve a mutually beneficial outcome.

(4) From the perspective of game theory, the bi-layer Stackelberg game has an advantage over the bi-layer mixed game, since each player has complete independence in decision-making. Through continuous information exchange and strategy adjustments, players can ensure that their own interests are maximized. Ultimately, the bi-layer Stackelberg game had the best overall performance. The net profit for NO and DGO increased by 85.17% and 36.00%, respectively. The charging cost for CA is reduced by a maximum of 37.90%, and renewable energy waste decreased by a maximum of 43.95%. Therefore, the bi-layer Stackelberg game is more conducive to improving the multidimensional benefits of a multi-participant system, positively promoting the enthusiasm of multi-operator participation in optimization, and providing more favorable operational strategies for different parties.

Limited by space and time, this paper did not consider the impact of ordered discharge on the optimization model, the influence of EV users' travel trajectories and traffic flow on charging demand, and the coordination between output deviation and charging plan adjustment during 15 min or even 5 min operation. These will be the directions of our future research.

Acknowledgement

This research was funded by The National Key Research and Development Program of China, grant number 2020YFB1707801, and The China Scholarship Council Joint Ph.D. Program, grant number CSC202206730084.

Appendix

A.1 Uncertainty modeling of wind and PV output

A.1.1 Wind output model

The uncertainty model of wind speed follows the Weibull distribution, which is given by

$$V(v)=\frac{k}{c}(\frac{v}{c})^{k-1}e^{-(\frac{v}{c})^{k}} \tag{A1}$$

where $V(v)$ is the wind speed model, v is the wind speed, and others are coefficients. The relationship between wind speed and wind power is formulated as follows:

$$P_{wp}(v(t))=\begin{cases}0, & v(t)<v_{i,w}, v(t)>v_{o,w}\\ \dfrac{g_r}{v_{r,w}^3-v_{i,w}^3}(v(t)^3-v_{i,w}^3), & v_{i,w}\le v(t)\le v_{r,w}\\ g_r, & v_{r,w}\le v\le v_{o,w}\end{cases} \tag{A2}$$

where $P_{wp}(v(t))$ is the available output of wind power units at time t, g_r is the rated output, $v_{i,w}$ and $v_{o,w}$ are the cut-in and cut-out wind speeds, $v_{r,w}$ is the rated wind speed, and $v(t)$ is the actual wind speed at time t.

A.1.2 PV output model

The output of a photovoltaic system generally follows the β distribution, which is given by

$$f(\theta)=\begin{cases}\dfrac{\Gamma(\alpha)\Gamma(\beta)}{\Gamma(\alpha)+\Gamma(\beta)}\theta^{\alpha-1}(1-\theta)^{\beta-1}, 0\le\theta\le1, \alpha\ge0, \beta\ge0\\ 0 \qquad\qquad\qquad\qquad\qquad\qquad, \text{others}\end{cases} \tag{A3}$$

where α and β are the shape parameters, and θ is the irradiation coefficient. Mean and standard deviation of irradiation are introduced to calculate the α and β, which are given by

$$\beta=(1-\mu)\times\left(\frac{\mu\times(1+\mu)}{\delta^2}-1\right) \tag{A4}$$

$$\alpha=\frac{\mu\times\beta}{1-\mu} \tag{A5}$$

where μ and δ are the mean and standard deviation of irradiation, the probability of solar irradiation state is given by

$$P(\theta)=\int_{\theta_c}^{\theta_d} f(\theta)d\theta \tag{A6}$$

where θ_c and θ_d are the bounds of θ. The output of photovoltaics is calculated by

$$P_{pv}(t)=\eta_{pv}\times S_{pv}\times\theta_t \tag{A7}$$

where η_{pv} is the output efficiency, S_{pv} is the total area of photovoltaic modules, and θ_t is the time exposed to sunshine.

A.1.3 Uncertainty modeling method

Scenario generation:

The uncertainty of wind and solar power can be transformed and solved through multi-scenario generation technology, and the Latin hypercube sampling method can be used to concentrate the samples in the high-probability space. The Latin hypercube sampling (LHS) method can stratify the cumulative probability curve and then obtain sample data, ensuring full coverage of the entire sample space. The flowchart of the LHS algorithm is shown in Figure A1.

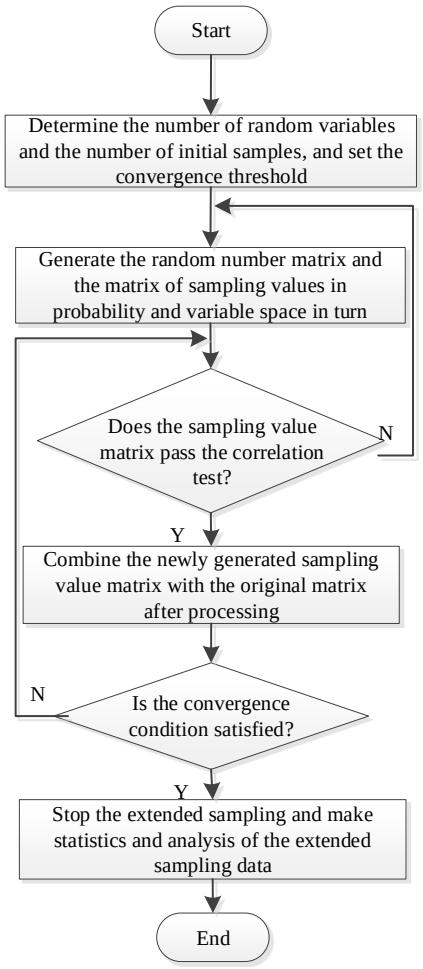

Figure A1 Steps of LHS algorithm

Scenario reduction:

To avoid generating too many scenarios during the scenario generation process, which may lead to complex and computationally intensive calculations, it is necessary to reduce similar scenarios. It is set that the generated number of samples is M, the number of target samples is M', the number of random variables is $X=[x_1,x_2,x_3,...,x_n]$, and the i-th sample is defined as $X_i=[x_1^i,x_2^i,x_3^i,...,x_n^i]$. Assuming that the initial probability of each scenario is

$$p_i=\frac{1}{M} \tag{A8}$$

1) Using scenario distance measurement to reduce similar scenarios by considering the average distance between scenarios:

$$s_{ij}=\sqrt{\sum_{y=1}^{n}[(X_{iw}-X_{jw})^2+(X_{iw}-\bar{X}_i)^2+(X_{jw}-\bar{X}_j)^2]} \tag{A9}$$

where $\bar{X}$ is the average distance between scenarios, X_{iw} and X_{jw} are the sample values in each scenario.

2) Removing the sample with the closest distance from the scenario set:

$$S_{ij} = p_j s_{ij} \tag{A10}$$

where p_j is the occurrence probability of scenario j, and s_{ij} is the distance between scenario i and scenario j.

3) Updating the probability of the occurrence of the sample:

$$p_i^{'} = p_i + p_j \tag{A11}$$

4) Repeating steps 1) to 3) until the number of scenarios is reduced to $M^{'}$.

A.2 Shapley-based benefit allocation model

The Shapley method is designed for solving the problem of benefit allocation under the cooperative operation of multiple entities [40]. Assuming that N is the set of stakeholders, and $v(S)$ represents the feature functions of *N*, the Shapley model is as follows:

$$\upsilon_i = \sum_{S \subseteq N} \frac{(|S|-1)!(n-|S|)!}{n!}(v(S)-v(S \setminus i)) \qquad \forall i \in N \tag{A12}$$

where υ_i is the allocated benefit of participant *i*, N is the participant set, $S \setminus i$ is the set of remaining entities except participant *i*.

References

[1] Chunyang Gong ZY, Hui Chen, Dongmei Huang, Xiaoliang Wang, Zhixin Wang, Shuai Shi. An optimal coordinated planning strategy for distributed energy station based on characteristics of electric vehicle charging behavior under carbon trading mechanism. International journal of electrical power & energy systems. 2023;147.

[2] Zhongfu Tan SY, Hongyu Lin, Gejirifu De, Liwei Ju, Feng'ao Zhou Multi-scenario operation optimization model for park integrated energy system based on multi-energy demand response. Sustainable cities and society. 2020;53:101973.

[3] Qingyou Yan HL, Jinmeng Li, Xingbei AI, Mengshu Shi, Meijuan Zhang, De Gejirifu. Many-objective charging optimization for electric vehicles considering demand response and multi-uncertainties based on Markov chain and information gap decision theory. sustainable cities and society. 2022;78.

[4] Liwei Ju XL, Shenbo Yang, Gen Li, Wei Fan, Yushu Pan, Huiting Qiao. A multi-time scale dispatching optimal model for rural biomass waste energy conversion system-based micro-energy grid considering multi-energy demand response. applied energy. 2022;327.

[5] Ning Li ZS, Houssem Jerbi, Rabeh Abbassi, Mohsen Latifi, Noritoshi Furukawa. Energy management and optimized operation of renewable sources and electric vehicles based on microgrid using hybrid gravitational search and pattern search algorithm. Sustainable cities and society. 2021;75.

[6] Khalil Gholami SK, Amjad Anvari-Moghaddam. Multi-objective Stochastic Planning of Electric Vehicle Charging Stations in Unbalanced Distribution Networks Supported by Smart Photovoltaic Inverters. Sustainable cities and society. 2022;84.

[7] Pouya Salyani M, Abapour, Kazem Zare. Stackelberg based optimal planning of DGs and electric

vehicle parking lot by implementing demand response program. Sustainable cities and society. 2019;51.
[8] Hongyu Lin XH, Pengshuo Yu, Qingyou Yan, Shenbo Yang, Mengshu Shi, Amjad Anvari-Moghaddam, Dong Liang. Multi-participant operation optimization for charging systems with orderly charging and cooperative game strategies considering carbon capture and uncertainties. journal of energy storage. 2023;59.
[9] Miriam Stumpe DR, Guido Schryen, Natalia Kliewer. Study on sensitivity of electric bus systems under simultaneous optimization of charging infrastructure and vehicle schedules. EURO Journal on Transportation and Logistics. 2021;10.
[10] CHANG Fangyu HM, ZHANG Weige. Research on Coordinated Charging of Electric Vehicles Based on TOU Charging Price. Power System Technology. 2016;40:2609-15.
[11] Enjian Yao TL, Tianwei Lu, Yang Yang. Optimization of electric vehicle scheduling with multiple vehicle types in public transport. Sustainable cities and society. 2020;52.
[12] Ning Li ZS, Houssem Jerbi, Rabeh Abbassi, Mohsen Latifi, Noritoshi Furukawa. Energy management and optimized operation of renewable sources and electric vehicles based on microgrid using hybrid gravitational search and pattern search algorithm. Sustainable cities and society. 2021;2021.
[13] Yanhui Cheng HZ, Ronaldo A. Juanatas, Mohammad Javad Golkar. Profitably scheduling the energy hub of inhabitable houses considering electric vehicles, storage systems, revival provenances and demand side management through a modified particle swarm optimization. Sustainable cities and society. 2023;92.
[14] Chanjuan Liu SSA, Alireza Rezvani, Sarminah Samad, Nahla Aljojo, Loke Kok Foong, Kentaro Nishihara. Stochastic scheduling of a renewable-based microgrid in the presence of electric vehicles using modified harmony search algorithm with control policies. Sustainable cities and society. 2020;59.
[15] LIN Mingrong HZ, GAO Mingxin, CHEN Jinpeng. Reliability evaluation of distribution network considering demand response and road-electricity coupling characteristics of electric vehicle load. Electric Power Construction. 2021;42:86-94.
[16] LI Hanyu DZ, CHEN Lidan, GUAN Lin, ZHOU Baorong. Trip simulation based charging load forecasting model and vehicle-to-grid evaluation of electric vehicles. automation of electric power systems. 2019;43:88-96.
[17] Wang Xi WW, Wang Haiyan, CChen Bo, Gou Jing, Li Yiran. Distributed two-stage shceduling strategy of EV considering user battery consumption. Electrical Measurement & Instrumentation. 2022;59:120-6.
[18] Lihua Lin SS, Yunlin Liao, Chuanliang Wang, Laleh Shahabi. Shunt capacitor allocation by considering electric vehicle charging stations and distributed generators based on optimization algorithm. energy. 2022;239.
[19] Ning Wang BL, Yan Duan, Shengling Jia. A multi-energy scheduling strategy for orderly charging and discharging of electric vehicles based on multi-objective particle swarm optimization. sustainable energy technologies and assessments. 2021;44.
[20] Lingyun Wang DW, Qiwei Ma, Jiayang Xu, Sheng Li. Double level optimal scheduling of electric vehicle charging and discharging with the best benefit of power plan, network and load. Renewable Energy Resources. 2018;36:713-8.
[21] Sun R. Coordinated charging strategies for electric vehicles considering interaction of "sourece-grid-load': Zhejiang university; 2018.
[22] Hou Hui XM, Chen Guoyan, Tang Jinrui, Xu Tao, Liu Peng. multi-objective hierarchical economic dispatch for microgrid considering charging and discharging of electric vehicles. Automation of electric

power systems. 2019;43:55-62.
[23] Miyu Yoshihara TN. Non-cooperative Optimization of Charging Scheduling for Electric Vehicle via Stackelberg Game and Matching Theory. IFAC-PapersOnLine. 2020;53-2:17029-34.
[24] Yeming Dai YQ, Lu Li, Baohui Wang, Hongwei Gao. A dynamic pricing scheme for electric vehicle in photovoltaic charging station based on Stackelberg game considering user satisfaction. computers & industrial engineering. 2021;154:107117.
[25] Songrui Li LZ, Lei Nie, Jianing Wang. Trading strategy and benefit optimization of load aggregators in integrated energy systems considering integrated demand response: A hierarchical Stackelberg game. energy. 2022;249.
[26] Kaijun Lin JW, Di Liu, Dezhi Li, Taorong Gong. Energy management optimization of micro energy grid based on hierarchical Stackelberg game theory. Power System Technology. 2019;43:973-81.
[27] Jiamei Li QA, Shuangrui Yin, Ran Hao. An aggregator-oriented hierarchical market mechanism for multi-type ancillary service provision based on the two-loop Stackelberg game. applied energy. 2022;323.
[28] Xi Luo YL, Jiaping Liu, Xiaojun Liu. Energy scheduling for a three-level integrated energy system based on energy hub models_ A hierarchical Stackelberg game approach. Sustainable cities and society. 2020;52.
[29] Mengmeng Yu SHH. Incentive-based demand response considering hierarchical electricity market_ A Stackelberg game approach. applied energy. 2017;203:267-79.
[30] Jian Ji MS, Benjamin Chris Ampimah. Design of virtual real-time pricing model based on power credit. Energy Procedia. 2017;142:2669-76.
[31] Cheng Sun SS, Xuanping Lai, Bin Zhu, YIfan Zhou, Tengfei Zhao. Economic dispatching strategy of grid-connected micro grid with electric vehicles based on virtual electricity price. Power Demand Side Management. 2021;23:79-83,95.
[32] Lu Xia JdH, Tansu Alpcan, Marcus Brazil, Doreen Anne Thomas, Iven Mareels. Local measurements and virtual pricing signals for residential demand side management. Sustainable Energy, Grids and Networks. 2015;4:62-71.
[33] Xiaodong Yang YZ, Guoqing Weng, Bo Zhao, Xiang Gao. Virtual Time-of-Use Tariffs Based Optimal Scheduling and Implementation Mechanism of Electric Vehicles Charging and Discharging. Transactions of China Electrotechnical Society. 2016;31:52-62.
[34] Qingshan Xu YY, Yu Huang, Jiankun Liu, Peng Wei. Probabilistic load flow computation using non-positive definite correlation control and latin hypercube sampling. High Voltage Engineering. 2018;44:2292-9.
[35] Li J. Research on the optimization model of purchase and sale of electricity retailers considering demand response: North China Electric Power University (Beijing); 2020.
[36] Shenbo Yang ZT, Jinghan Zhou, Fan Xue, Hongda Gao, Hongyu Lin, Feng'ao Zhou. A two-level game optimal dispatching model for the park integrated energy system considering Stackelberg and cooperative games. International journal of electrical power & energy systems. 2021;130.
[37] Shenbo Yang ZT, Shuaiyu Gou, Peng Li, Liwei Ju, Feng'ao Zhou, Xing Tong. Optimization model of WPO-PVO-ESO cooperative participation in day-ahead electricity market transactions considering uncertainty and CVaR theory. international journal of electrical power & energy systems. 2021;129.
[38] Transportation USDo. National Household Travel Survey. In: Transportation USDo, editor.2017.
[39] Song Y. Energy consumption modeling and cruising range estimation based on driving cycle for electric vehicles: Beijing Jiaotong University; 2014.
[40] TAN Zhongfu TC, PU Lei, YANG Jiacheng. Two-layer game model of virtual power plant applying

CIQPSO algorithm. Electric Power Construction. 2020;41:9-17.
[41] Xiaojuan Han ZW, Zhenpeng Hong, Song Zhao. Ordered charge control considering the uncertainty of charging load of electric vehicles based on Markov chain. renewable energy. 2020;161:419-34.
[42] Wang Y. Research on multi-energy collaborative optimization operation and benefit evaluation model of micro energy grids: North China Electric Power University; 2020.
[43] Yanbo Liu XQ, Gao Qiu. Optimal operation of micro grid account of the response of electric vehicle user. High Voltage apparatus. 2016;52:0163-9.
[44] Hongyu Lin QY, Xueting Li, Jialu Dang, Shenbo Yang, De Gejirifu, Lujin Yao, Yao Wang. Multi-energy coordinated and flexible operation optimization and revenue reallocation models for integrated micro energy system considering seasonal and daily load characteristics of different buildings. energy reports. 2022;8:12583-97.